2017197

by Aeron Smitham

Submission date: 08-Mar-2024 10:45PM (UTC+0000)
Submission ID: 226141352
File name: 16679_Aeron_Smitham_2017197_180903_135059343.pdf (5.81M)
Word count: 10659
Character count: 65981

Course:	BSc (Hons) Electrical and Electronic Engineering
Module:	SGEE6001 Power Electronics and Drives
Assignment:	Investigation into DC drives and control methods
Name:	Aeron Smitham
University number:	2017197
Date submitted:	08/03/2024
Word count:	3283

Table of Contents

Table of Figures 4

Table of Tables 6

Table of Equations 7

1. Executive Summary 8

2. Work plan for Life-long Learning 9

3. Research 10

3.1. Design Features and Control Techniques in a 4-Quadrant 3-Phase DC Drive 10

3.1.1. Speed Control Loop 10

3.1.2. Four-Quadrant Drives 13

3.2. DC Drive Specification 15

3.3. Applications of 4-Quadrant DC Drives (Comparing with single-phase converters and chopper drives, and AC drives) 18

4. Simulation and Design Adaption 19

4.1. Three Phase Full Wave Controlled Rectifier 19

4.1.1. 10° Firing Angle Test and Result Table 21

4.2. Design Adaption 23

4.2.1. 4-Quadrant Operation 25

5. Practical Investigations 26

5.1. Practical Task Setup 26

5.2. 4-Quadrant Operation 28

5.3. Speed Setpoints with Constant Torque DC Motor Analysis 33

5.3.1. 1000RPM Test & Calculations 33

5.3.2. Discontinuous Current Speed Setpoint Test Results 36

5.3.3. DC Motor Constants 37

5.4. Continuous Current Torque Setpoints DC Motor Analysis 40

6. Conclusions and Recommendations 42

7. References 44

8. Appendix 46

8.1. Appendix for Section 3 46

8.1.1. Design Features & Control Techniques Supporting Evidence 46

8.1.2. DC Drive Specification 48

8.1.3. Applications of 4-Quadrant DC Drives 52

8.2. Appendix for Section 4 53

8.2.1. Three Phase Full Wave Controlled Rectifier Supporting Evidence 53

8.2.2. Design Adaption Supporting Evidence 59

8.3. Appendix for Section 5 62
8.3.1. Practical Task Supporting Evidence 62
8.3.2. Practical 4-Quadrant Operation Supporting Evidence 63
8.3.3. Discontinuous Current Speed Setpoint Test Supporting Evidence 71
8.3.4. Torque Setpoint Test at Constant Speed Supporting Evidence 76

A very detailed and professional table of contents

Table of Figures

Figure 1 – Speed Control Loop (Rashid, 2013) 10
Figure 2 – DC Drive Base Speed & Above Base Speed Graph (MathWorks, 2024) 12
Figure 3 – Four Quadrant Graph (Rashid, 2013) 13
Figure 4 – Four Quadrant Speed & Armature Current Operation Graph with Quadrants Labelled (Rashid, 2013) 14
Figure 5 – Minimum Connection Requirements for Parker 590+ Operation (Parker, 2024) 15
Figure 6 – Speed Control Loop of Parker 590+ DC Drive with Annotation (Parker, 2024) 17
Figure 7 – Annotated 3-Phase Full Wave Controlled Rectifier Multisim Circuit 19
Figure 8 - 10° Firing Angle Multisim Graph 21
Figure 9 – Circuit Design Adaption Dual Converter 23
Figure 10 – Isolating Transformers and Snubber Networks of Design Adaption Circuit 24
Figure 11 – Four Quadrant Operation with All Four Quadrants Displayed on Graph 25
Figure 12 – AC-DC Motor System Setup with Annotations 26
Figure 13 – Fluke 325 Clamp Meter with Annotations 27
Figure 14 – Four Quadrant Operation on HMI Trace with Annotations 28
Figure 15 – Four Quadrant Operation on Picoscope Displayed Graphically 29
Figure 16 – 1000RPM Picoscope Graph 33
Figure 17 – 1000RPM HMI Result 33
Figure 18 – Picoscope DC Motor Constant Values 37
Figure 19 – Picoscope Cursor Values 37
Figure 20 – HMI DC Motor Constant Values 38
Figure 21 – Picoscope Result at 6Nm 40
Figure 22 – HMI Result at 6Nm 40
Figure 23 – Torque & Power Characteristics Up to & Above Base Speed (Rashid, 2013) 46
Figure 24 – Field Weakening Control Loop (Rashid, 2013) 47
Figure 25 – Dual Converter DC Drive (Rashid, 2013) 47
Figure 26 – Current Control Loop of Parker 590+ DC Drive (Parker, 2024) 48
Figure 27 – Electrical Schematic of Parker 590+ DC Drive (Parker, 2024) 49
Figure 28 – Parker 590+ Labelled Description of Unit (Parker, 2024) 50
Figure 29 – Parker 590+ Field Weakening Control Loop (Parker, 2024) 51
Figure 30 – 4-Quadrant Operation of an Elevator (Invertek Drives , 2024) 52
Figure 31 – Firing Angle set to 0° 53
Figure 32 – Back EMF Polarity Reversed with Firing Angle set to 90° 54
Figure 33 – Single Converter with Quadrant 4 Operation 54
Figure 34 – Firing Angle set to 20° 55
Figure 35 – Firing Angle set to 30° 56
Figure 36 – Firing Angle set to 40° 57
Figure 37 – Firing Angle set to 50° 58
Figure 38 – Converter 2 Connected 59
Figure 39 – Gate Triggers for Converter 2 59
Figure 40 – Quadrant 1 Multisim Graph 60
Figure 41 – Quadrant 2 Multisim Graph 60
Figure 42 – Quadrant 3 Multisim Graph 61
Figure 43 – Quadrant 4 Multisim Graph 61
Figure 44 – Control Cabinet with Drives, PLC & HMI 62
Figure 45 – Fluke & Picoscope Clamp Meters 62

Figure 46 – Quadrant 1 HMI Result 63
Figure 47 – Quadrant 1 Picoscope Result 63
Figure 48 – Quadrant 1 Fluke Result 64
Figure 49 – Quadrant 2 HMI Result 65
Figure 50 – Quadrant 2 Picoscope Result 65
Figure 51 – Quadrant 2 Fluke Result 66
Figure 52 – Quadrant 3 HMI Result 67
Figure 53 – Quadrant 3 Picoscope Result 67
Figure 54 – Quadrant 3 Fluke Result 68
Figure 55 – Quadrant 4 HMI Result 69
Figure 56 – Quadrant 4 Picoscope Result 69
Figure 57 – Quadrant 4 Fluke Result 70
Figure 58 – Vmax at 591V from Picoscope 71
Figure 59 – Picoscope Graph Annotated for Mathematical Terms 71
Figure 60 – 1400RPM Picoscope Results 72
Figure 61 – 1400RPM HMI Result 72
Figure 62 – 1800RPM Picoscope Result 74
Figure 63 – 1800RPM HMI Result 74
Figure 64 – 4.5Nm Picoscope Result 76
Figure 65 – 4.5Nm HMI Result 76
Figure 66 – 3Nm Picoscope Result 77
Figure 67 – 3Nm HMI Result 77

An extensive and detailed table of figures

Table of Tables

Table 1 – Four Quadrant Table with Speed, Torque & Power Conditions (Circuit Globe, 2017) 13
Table 2 – Parker 590+ DC Drive Specification (Parker, 2024) 15
Table 3 – Parker 590+ DC Drive IO Terminal Descriptions (Parker, 2024) 16
Table 4 – DC Drive & Motor Benefits 18
Table 5 – 3-Phase Rectifier Firing Angle Test Results 22
Table 6 – Four Quadrant Operation Expected Result Compared with Simulated Result 25
Table 7 – Picoscope Key 29
Table 8 – Four Quadrant Operation Comparison Between Expected, HMI & Picoscope Results 30
Table 9 – Four Quadrant Operation HMI Drive Values 30
Table 10 – Armature Voltage & Current Comparison Between HMI, Fluke Clamp & Picoscope 32
Table 11 – 1000RPM Calculation Values 34
Table 12 – Discontinuous Current Speed Test 35
Table 13 – Discontinuous Current Speed Test Results 36
Table 14 – Continuous Current Torque Setpoint Results 41
Table 15 – Figure 28 Key 50
Table 16 – Values for 1400RPM Calculations 73
Table 17 – 1800RPM Calculation Values 75

Good extensive use of tables to order and evaluate results

Table of Equations

Equation 1 – Peak Voltage 20
Equation 2 – Vmean 20
Equation 3 – Vmean Result 21
Equation 4 – Area A Calculation 34
Equation 5 – Area B Calculation 34
Equation 6 – Vmean Calculation 34
Equation 7 – $1000RPM\ \alpha\ Calculation$ 34
Equation 8 – 1000RPM Area A Calculation Result 34
Equation 9 – 1000RPM Area B Calculation Result 34
Equation 10 – Vmean Calculation Result 35
Equation 11 – Armature Voltage Calculation 37
Equation 12 – Armature Resistance Calculation 38
Equation 13 – Armature Voltage Calculation Result 38
Equation 14 – DC Motor Torque Constant 39
Equation 15 – Back EMF Constant 39
Equation 16 – Ke Constant 39
Equation 17 – Vmean Result at 20° 55
Equation 18 = Vmean Result at 30° 56
Equation 19 – Vmean Result at 40° 57
Equation 20 – Vmean Result at 50° 58
Equation 21 – $1400RPM\ \alpha\ Calculation$ 73
Equation 22 – 1400RPM Area A Calculation Result 73
Equation 23 – 1400RPM Area B Calculation Resul 73
Equation 24 – 1400RPM Vmean Calculation Result 73
Equation 25 – 1800RPM α Calculation Result 75
Equation 26 – 1800RPM Area A Calculation Result 75
Equation 27 – 1800RPM Area B Calculation Result 75
Equation 28 – 1800RPM Vmean Calculation Result 75

Good use of tables to logically order results

1. Executive Summary

This assignment has successfully encompassed comprehensive research, simulation, and practical testing concerning DC drives and their control methods. The research delved into advanced power electronic circuits, electrical machines, and drive systems, applying the derived theories to simulations and practical tasks. Specific attention was given to the design features and control techniques of a three-phase, four-quadrant DC drive, focusing on speed and armature current feedback within the control loop.

An in-depth examination of the Parker 590+ Series DC drive provided insights into its specifications, operational requirements, and characteristics. The research also explored the typical applications of four-quadrant DC motors, emphasizing scenarios where they outperform their AC counterparts, such as in cranes and hoists requiring precise control at low speeds. *Good points made here*

The subsequent simulation in NI Multisim modelled a separately excited DC motor controlled via a three-phase fully-controlled full-wave rectifier. The simulation validated the expected results, demonstrating the inverse relationship between firing angle and armature voltage. Comparisons between simulated and calculated values revealed negligible errors, affirming the effectiveness of the simulation model. *Good observation*

Adapting the original simulation to operate in all four quadrants further demonstrated its versatility, with oscilloscope measurements confirming accurate waveforms in each quadrant. Practical investigations with the Siemens DC drive and AC motor in all four quadrants corroborated theoretical expectations. The HMI trace graph, Picoscope waveforms, and a Fluke 325 current clamp meter provided accurate performance data, validating the proportional relationships between armature voltage and speed, as well as between torque and current. *Good points made*

Two additional practical tests, focusing on speed variations and torque adjustments, further supported the established relationships. This cohesive outcome underscores the precision and reliability of the theory, simulations, and practical experiments conducted throughout the assignment. *A very well written summary*

2. Work plan for Life-long Learning

A comprehensive work-plan is essential, to successfully approach this assignment, which includes the research, simulation, and practical investigation into DC drives and their control methods, specifically focussing on four-quadrant operation and the associated effects this has on motor armature voltage and current.

The first phase involves a detailed literature review to establish a good theoretical knowledge of the design features and control techniques of a four-quadrant DC drive, the specification of a modern DC drive, and its typical applications when compared with such drives as a modern AC Variable Frequency Drive (VFD). The research will inform the next steps, laying the foundation for theoretical predictions.

Once the research has been completed, attention changes to the simulation task. NI Multisim will be used to build and test the three-phase full-wave controlled rectifier, including the effects that the firing angle has on armature voltage applied to the motor. Calculations will be completed to compare mathematical results with the simulated results. The circuit will then be adapted to run in all four quadrants and the results will be compared from the various test equipment used.

The practical task will involve a series of experiments utilising the Siemens three-phase DCM drive and the Siemens S120 AC drive – which serves as the motor load. The HMI screen will be used to control and monitor the system, with the Picoscope recording data and displaying the resultant waveforms. The operation of the drive in all four quadrants will be demonstrated and comparisons between the comparison and the theory will be made. A second test demonstrating discontinuous current for three different speed values at a constant torque will be completed, with the relationship between armature voltage and speed discussed. A similar test will be undertaken, with three torque setpoints at constant speed investigated and the relationship between torque and current examined.

With the report complete, it can be seen that the work-plan was successfully followed, with each task completed. The report shows a detailed understanding gained from the research, with this knowledge then applied to the simulation and practical tasks.

Good plan with significant details

3. Research

3.1. Design Features and Control Techniques in a 4-Quadrant 3-Phase DC Drive

3.1.1. Speed Control Loop

The speed control loop of a DC drive is a crucial component that regulates the motor speed to meet desired specifications. The speed control loop typically involves a feedback system that continuously monitors the motor speed and adjusts the control signal to maintain the desired speed. An example with a speed feedback, current feedback and field control loop can be seen in figure 1.

Internal control loops are identified here and with a good supporting diagram

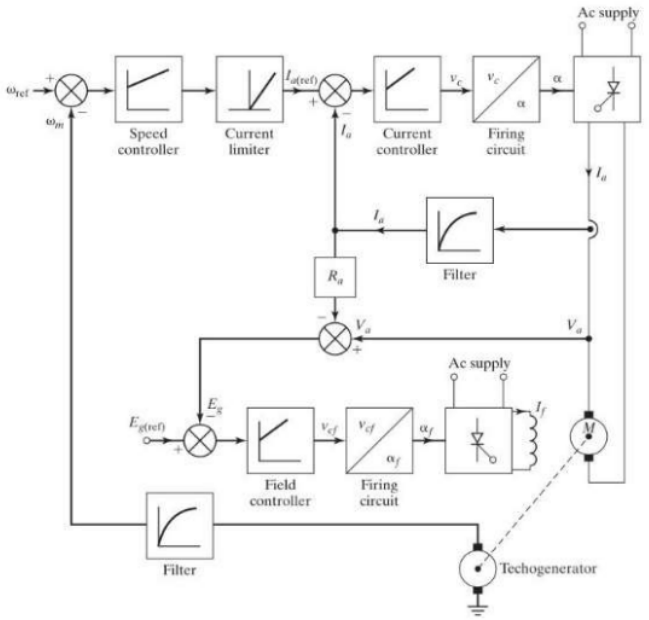


Figure 1 – Speed Control Loop (Rashid, 2013)

The speed control loop requires a sensing component, such as an encoder or tachometer, which can be used to continuously feedback the motors actual speed to the reference speed comparator of the control loop. The reference speed, either set manually or automatically, is entered into the comparator as the speed setpoint of the motor and from this, an error calculation is performed between the reference speed and the actual speed. The outcome of this calculation generates an error signal, representing how much the motor speed deviates from the reference speed (Krishnan, 2001).

Good significant point

Very good work with good ref source

The error signal is then processed by a speed controller and limiter block, for instance a PI (Proportional-Integral) or PID (Proportional-Integral-Derivative) controller. The motor speed can then be increased or limited, dependant on the reference speed. The proportional component responds to the current error, the integral component considers accumulated past errors, and the derivative component anticipates future errors based on the rate of change. The speed control block then generates a reference current based on the difference between the reference and actual speed (Rashid, 2014). *This is very good work with PID control and purpose of error explained*

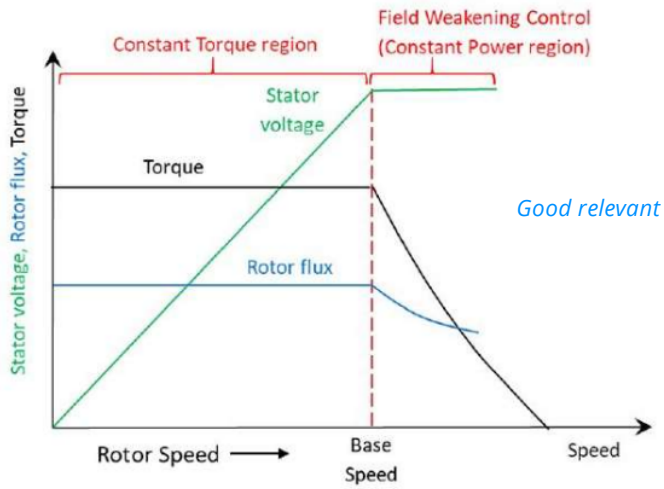
The reference current is used as a control signal into a second comparator that compares this signal and the armature current feedback of the motor. If there is an error between the two currents, then a second current controller can rectify this by altering the current to the armature of the motor. Conversely, if there is no error, then the same amount of current will be supplied to the motor (Mohan & Undeland, 2003). *Good points*

The controlled current signal is sent to the firing control and pulse amplifier which controls the firing angle of the thyristors in the converter. The firing angle signal is sent to the converter, which then controls the firing angle of the thyristors which, in turn, controls the speed of the motor by altering the armature voltage (Lander, 1993). *Good work with purpose of firing angles explained*

The process repeats continuously in a closed-loop fashion. The speed sensor continually provides feedback to the control system, allowing real-time adjustments to maintain the desired speed, even in the presence of external disturbances or changes in load. *Good point*

By continuously adjusting the control signal based on the feedback from the speed sensor, the speed control loop ensures that the DC motor operates at the specified speed under varying conditions, providing a stable and responsive control system. *A very significant point*

Armature voltage feedback and field weakening are two forms of speed control for a DC motor. Figure 2 shows a graph detailing the performance of a DC motor up to and above base speed. Up to base speed, the torque is constant, field flux remains constant, and the armature voltage increases linearly with speed. Once the field flux reduces, there is an exponential torque decay above base speed. Further investigation into these methods can be seen in section 8.1.1 in the appendix. *Good explanation*



Good relevant diagram

Figure 2 – DC Drive Base Speed & Above Base Speed Graph (MathWorks, 2024)

3.1.2. Four-Quadrant Drives

A four-quadrant DC drive is a versatile electronic control system used to regulate the speed and direction of a DC motor in various operating conditions. The four quadrants refer to different combinations of motor speed and direction, creating a dynamic control system capable of both motoring and regenerative braking (Krishnan, 2001).

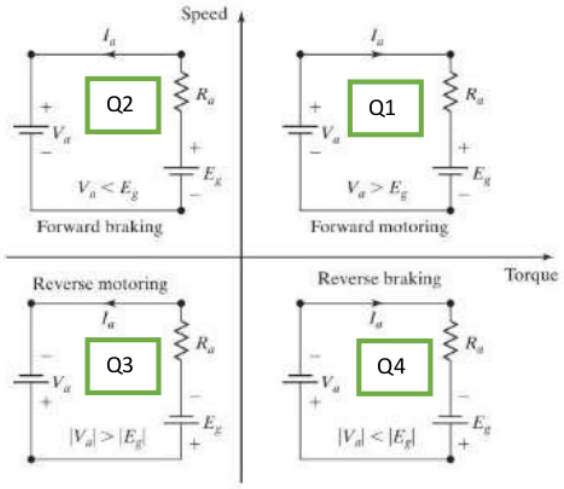


Figure 3 – Four Quadrant Graph (Rashid, 2013)

Good explanation with very good relevant diagram and ref source

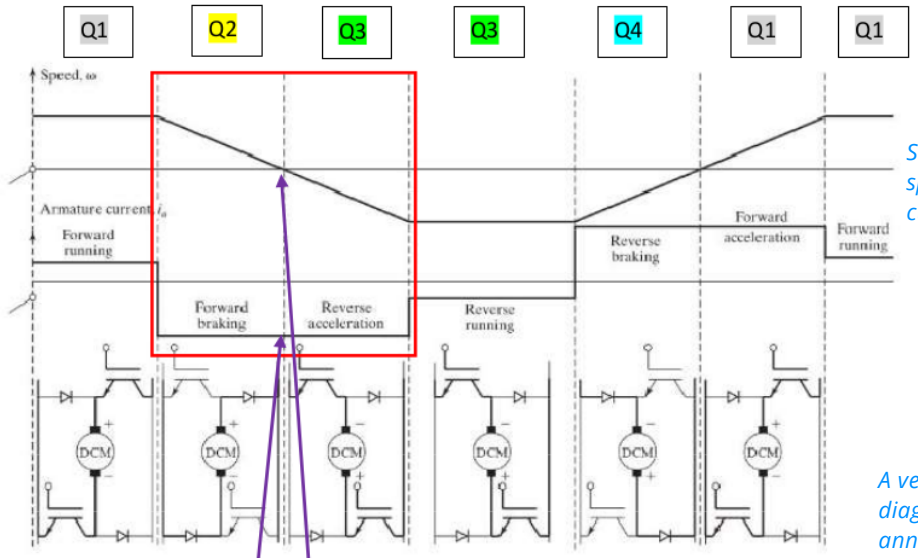
In figure 3, each quadrant can be seen. The forward motoring of Q1 can be achieved with positive voltage and current. The forward braking of Q2 can be achieved with positive voltage and negative current. The reverse motoring of Q3 can be achieved with negative voltage and current, with the reverse braking of Q4 achieved with negative voltage and positive current. Table 1 shows the speed and torque equivalent conditions of a 4-quadrant drive, which matches the theory of figure 3 by showing the relationship between speed and armature voltage, and torque and current.

Function	Quadrant	Speed	Torque	Power Output
Forward Motoring	I	+	+	+
Forward Braking	II	+	-	-
Reverse Motoring	III	-	-	+
Reverse Braking	IV	-	+	-

Table 1 – Four Quadrant Table with Speed, Torque & Power Conditions (Circuit Globe, 2017)

Good use of table to identify speed and torque in 4 quadrant drive scenario

Figure 4 shows the speed and armature current of a DC motor in 4-quadrant operation. The sections have been annotated to show their quadrant of operation. The red highlighted section covers the forward braking of Q2 as the speed decreases from Q1 and the current going negative, and then the current remaining negative while speed becomes negative as the motor moves into Q3.



Significant events for speed and armature current identified

A very good detailed diagram with good annotations.

Figure 4 – Four Quadrant Speed & Armature Current Operation Graph with Quadrants Labelled (Rashid, 2013)

The two arrow points of the graph show where the speed becomes negative and where current is still negative – signalling the change into Q3.

3.2. DC Drive Specification

The specification for a Parker 590+ series drive has been investigated with the details of the drive shown in table 2.

Parker 590+ *590P-53.2350.1.0.P.00.U.4.A.E* DC Drive Specification		
Specification	**Value**	**Part Number**
Regenerative/Non-Regen	Regenerative	590P
Supply Voltage	220-500VAC	53
Output Current	35A	2350
Frame Size	1	1
Auxiliary Supply	115-230VAC	0
Mechanical Style	Panel Mounting	P
Special Option	None	00
Language	English	U
Keypad	6901 Keypad Fitted	4
Speed Feedback	Analog Tacho	A
Comms	Ethernet	E
Power	15kW	-
Motor HP	20HP	-
Field Current	4A	-

Table 2 – Parker 590+ DC Drive Specification (Parker, 2024)

Figure 5 shows the minimum connection requirements for the Parker 590+ drive to run. *Good significant point*

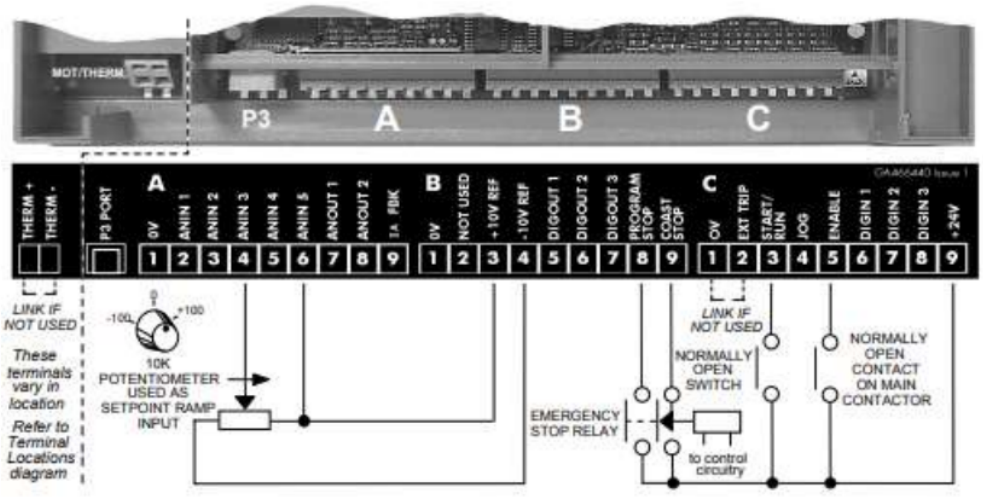


Figure 5 – Minimum Connection Requirements for Parker 590+ Operation (Parker, 2024)

A good level of detail included in the spec here and good use of table

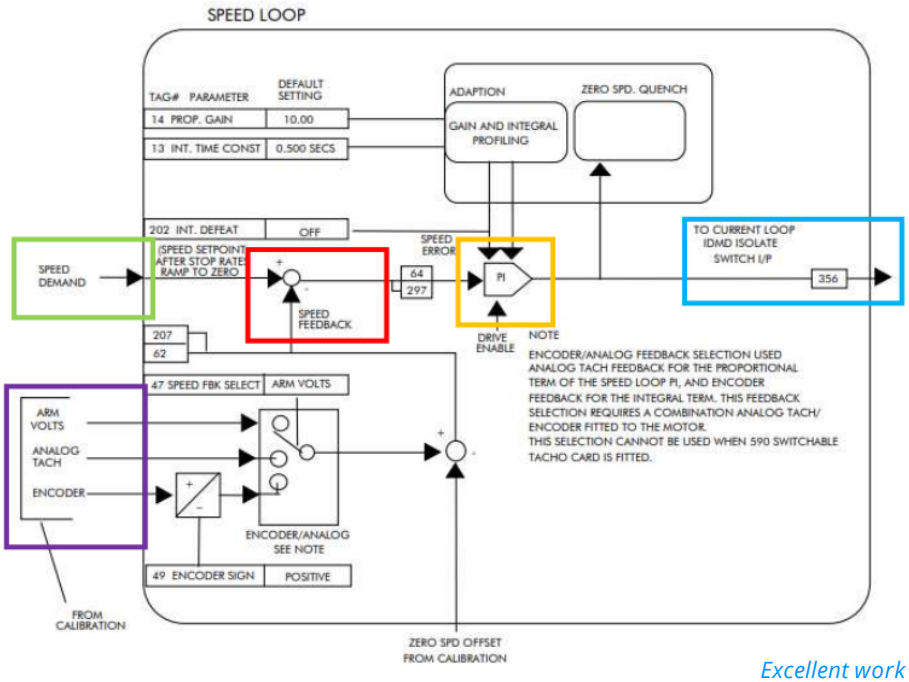
Table 3 details what the function of the terminals are in figure 5.

Parker 590+ DC Drive IO Terminal Connections		
Terminal	**Name**	**Function**
C9	+24V	24VDC output from drive to be used as the dedicated supply for the inputs into the drive.
C5	Enable	C5 is connected to C9 (+24V) through a normally open contact on the main drive supply contactor. The drive will remain disabled until the main contactor is closed.
C4	Jog	This is a one-button function for positioning the motor at a pre-determined speed.
C3	Start/Run	Connect terminal C3 (RUN) to C9 (+24V) through a normally open contact. This provides normal start/stop control. When it is closed, the drive will start; when the contact is open, the drive will attempt to perform a controlled stop.
C2	Ext Trip	This input terminal provides an external trip facility to any normally closed trip switch. For example, if the motor has an external blower motor, wire an auxiliary contact from the blower starter's overload trip circuitry between terminals C1 and C2.
B8 & B9	Stop	For a regenerative emergency stop connect terminal B8 to terminal C9 through a normally open contact of an emergency stop relay. Also connect terminal B9 to terminal C9 through a time-delayed off, normally open contact on the same emergency stop relay. Activating the E-Stop circuit removes 24 VDC from B8 and regenerates the motor power back into the main supply. The delayed-off contact on B9 acts as a fail-safe, allowing the drive to coast to stop after the time delay.
A4, B3 & B4	Speed Demand	For normal operation, connect the speed demand signal to terminal A4. This input is scaled so that +10VDC input equals the maximum forward speed demand (+100%), and -10VDC input equals the maximum reverse speed demand (-100%). Connect the ends of an external potentiometer to terminals B3 (+10VDC REF) and B4 (-10VDC REF) and the wiper to terminal A4.
A6	Current Limit	For most applications, connect terminal A6 to terminal B3 (+10VDC REF). This sets the drive's positive and negative current limit to +100% and -100% respectively for forward and reverse motor operation. This allows the main current limit to be controlled internally, via the Keypad, using the MAIN CURRENT LIMIT parameter. To control the main current limit externally, connect a 10kΩ potentiometer between terminals B3 (+10VDC REF) and B1 (0VDC). Connect the wiper to terminal A6 instead of the connection above. The potentiometer will now control the current limit from 0 to 200% if the MAIN CURRENT LIMIT parameter is set at 200.00%

Table 3 – Parker 590+ DC Drive IO Terminal Descriptions (Parker, 2024)

Good work

Figure 6 shows the speed loop of the Parker 590+ DC drive, with a signal from the speed demand, highlighted in green. The speed feedback signal in to the comparator can be seen in red, with the options of what speed feedback can be used highlighted in purple. The options given for speed feedback are armature voltage, tacho or encoder. The speed PI controller can be seen in orange, which has 4 inputs – a speed error, proportional gain, integral time constant, and drive enable signal. The PI speed controller has an output signal to the current loop, highlighted in blue, that is detailed in figure 26 in section 8.1.2 of the appendix.



Excellent work here

Figure 6 – Speed Control Loop of Parker 590+ DC Drive with Annotation (Parker, 2024)

3.3. Applications of 4-Quadrant DC Drives (Comparing with single-phase converters and chopper drives, and AC drives)

Direct current (DC) motors and drives offer several advantages over their alternating current (AC) equivalents in certain applications. Table 4 details the benefits of DC drives, when compared with other options.

Benefits	Description
Precise Speed Control	DC motors provide precise and adjustable speed control. This makes them suitable for applications where speed variations are critical, such as in robotics, conveyor systems, and certain manufacturing processes.
High Starting Torque	DC motors typically have high starting torque, making them well-suited for applications that require a quick and powerful start, such as in electric vehicles and certain industrial machinery.
Simple Speed Regulation	DC drives offer a straightforward method of controlling motor speed through simple adjustments in the applied voltage. This simplicity can be advantageous in applications where frequent speed changes are required.
Efficiency in Variable Speed Applications	DC motors and drives can be more efficient than AC motors in variable speed applications, especially when precise control over speed and torque is essential. This efficiency is crucial in applications like traction control in electric vehicles.
Ease of Reversal	DC motors can easily change direction by simply reversing the polarity of the applied voltage. This feature simplifies the control system design and is advantageous in applications where frequent changes in rotation direction are needed.
Compact Size and Weight	DC motors are generally smaller and lighter than their AC counterparts with similar power ratings. This compactness makes them suitable for applications with space constraints, such as in portable devices and smaller machinery.
Regenerative Braking	DC drives allow for regenerative braking, where energy generated during braking is fed back into the power supply. This regenerative capability contributes to increased energy efficiency and can be important in applications with frequent stops and starts.
Cost-Effective for Small to Medium Applications	In certain power ranges, DC motors and drives can be more cost-effective than their AC counterparts. This cost advantage is particularly notable in smaller to medium-sized applications where the complexity of AC systems may not be necessary.
Widely Used in Existing Installations	DC motors have been traditionally used in various industries, and there are still many existing installations with DC systems. In such cases, upgrading to newer DC drives may be more practical than transitioning to entirely new AC systems.

Table 4 – DC Drive & Motor Benefits (Wildi, 2014) & (Wilamowski & Irwin, 2017)

Very good comparison table that highlights significant advatages for DC motors

An application of a DC motor can be seen in section 8.1.3. of the appendix.

Chopper fed drives should be included in the comparison

4. Simulation and Design Adaption

4.1. Three Phase Full Wave Controlled Rectifier

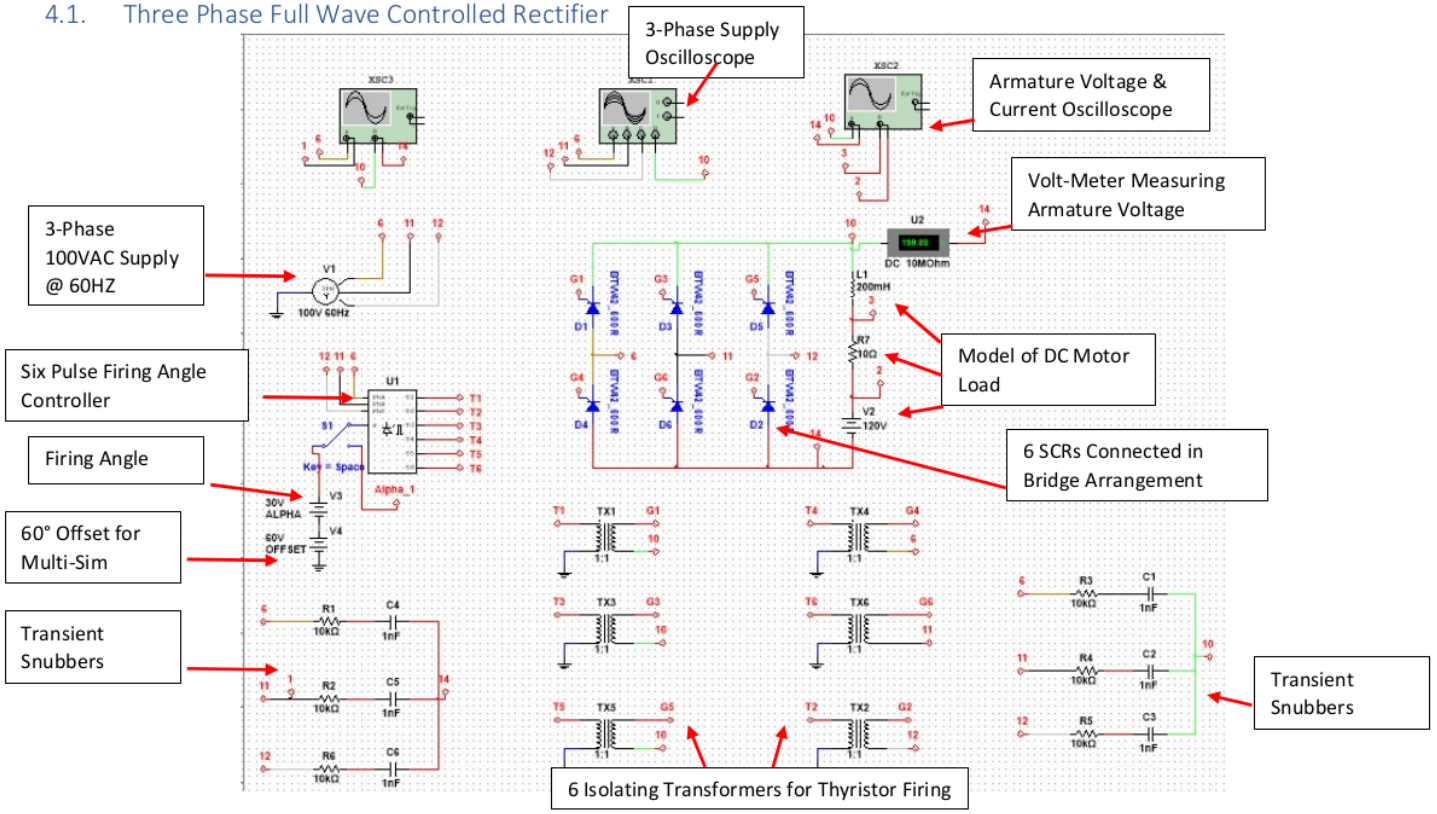


Figure 7 – Annotated 3-Phase Full Wave Controlled Rectifier Multisim Circuit

Excellent annotated sim diagram that identifies key features

Figure 7 displays an annotated picture of the three-phase full-wave controlled rectifier circuit on NI Multi-Sim which models a separately excited motor, with the model containing a resistor (R7), inductor (L1) and back EMF (V2).

The firing angle of the thyristors are controlled via a 6-pulse phase angle controller which outputs each signal to its own 1:1 ratio isolating transformer to isolate the motor from the incoming supply. The Silicon Controlled Rectifier (SCR) gates are triggered by the signal from the secondary side of the isolating transformers. The SCRs are connected in three sets of pairs in a bridge arrangement.

A battery (V3) is connected to the alpha terminal of the firing angle controller to set the firing angle, as the voltage of the battery equates to the firing angle e.g. 50V = 50°. There is also a second battery (V4), that gives a 60V offset to the firing angle controller as this is required due to issues with NI Multisim. *Good significant point*

There are also transient snubber networks, consisting of resistors and capacitors, which are connected in parallel with the SCRs to limit transient voltage surges. The thyristors used have a breakdown voltage of 600V and the Multisim circuit has a peak voltage of 141V, which is well within the safe working range. The peak voltage can be found via equation 1.

$$Peak\ Voltage = 100V \times \sqrt{2} = 141V$$

Good work

Equation 1 – Peak Voltage

With the firing angle set to 0°, V_{max} is found via a cursor on Multisim to be 242V, which can be seen in figure 31 in appendix section 8.2.1. V_{max} can then be used in equation 2 to calculate the mean armature voltage with different firing angles and the result will be compared with a simulated value on NI Multisim.

$$V_{mean} = \frac{3 \times V_{max}}{\pi} \times Cos(\alpha)$$

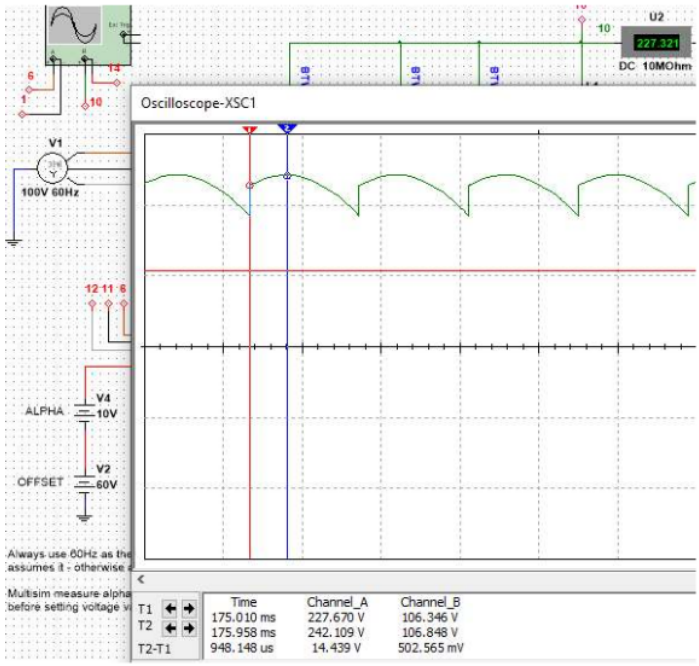
Correct equation is identfied

Equation 2 – Vmean

The circuit was modified to run in quadrant 4, by reversing the polarity of the back EMF (V2) and increasing the firing angle above 90°. The result of this is voltage goes negative, while current remains positive, simulating the motor running in forward regeneration. The modified circuit can be seen in figure 32 in appendix 8.2.1. *Good explanation*

4.1.1. 10° Firing Angle Test and Result Table

Figure 8 shows the first test carried out, with the firing angle set to 10°. The armature voltage can be seen to be 227.32V on the voltmeter. In figure 8, the current is continuous at a firing angle of 10°. The green trace is voltage, with the red trace representing current.



Good test result

Figure 8 - 10° Firing Angle Multisim Graph

Equation 2 can then be used to find the calculated value of the armature voltage, with Vmax = 242V and $\alpha = 10°$ substituted into equation 3.

$$V_{mean} = \frac{3 \times 242}{\pi} \times Cos(10) = 227.58V$$

Good result

Equation 3 – Vmean Result

A further four tests were carried out, with the firing angle set to 20°, 30°, 40° and 50°. The simulated and calculated results for these tests can be seen in table 5. Evidence for these tests can be seen in section 8.2.1 of the appendix.

3-Phase Rectifier Firing Angle Tests				
Alpha α	Armature Mean Voltage (V)		Error	Figure
	Simulated Voltage	Calculated Voltage		
10	227.32V	227.58V	0.26	8
20	217V	217.16V	0.16	34
30	199.9V	200.13V	0.14	35
40	176.76V	177.03V	0.27	36
50	148.36V	148.54V	0.18	37

Good table of results with error identified

Table 5 – 3-Phase Rectifier Firing Angle Test Results

The simulated and calculated results in table 5 have proven successful, with only a minor error between both results for each separate firing angle. The largest error of 0.27 was for 40°, while the smallest error is 0.14 for 30°. There is no correlation between the errors, as the firing angle is increased, so the issue is likely to be with the either mathematical rounding errors, volt drop across the thyristors in Multisim, or the time at which the simulated snapshot value was taken.

Good argument for error correlation

With both test methods, simulation and calculation, the relationship between firing angle and voltage can be seen. As the firing angle increases, the voltage begins to decrease, as the full wave is being 'chopped' and part of the wave is not being utilised.

Good explanation of results

4.2. Design Adaption

As seen in section 4.1, the full-wave three phase rectifier can only operate in quadrants 1 and 4. To allow four quadrant operation, the circuit must be modified to a three-phase dual rectifier which adds a second SCR bridge which is connected in anti-parallel across the other side of the load so it can provide negative current. *Good point*

Figure 9 displays the modified circuit with dual-bridge rectifiers. Bridge 1 runs the motor in quadrant 1 when the firing angle is below 90°, and in quadrant 4 when the firing angle is above 90°. Bridge 2 runs the motor in quadrant 3 when the firing angle is below 90°, and in quadrant 2 when the firing angle is above 90°. The circuit is much the same as before but with 4 single-pole single-throw (SPST) switches for each bridge rectifier. When bridge 1 is in operation, SPST 4, 5, 14 and 15 are closed, with the other 4 switches open, and when bridge 2 is in operation, SPST 6, 7, 8 and 16 are closed, with the other four switches open. Figure 9 has been annotated to explain these points further. *Good detailed explanation*

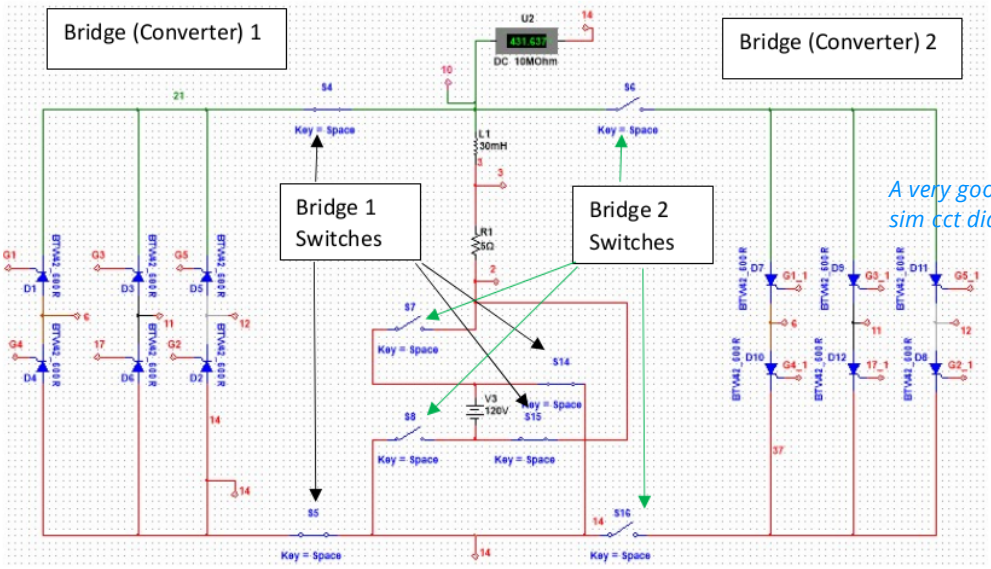


Figure 9 – Circuit Design Adaption Dual Converter

Figure 10 shows the isolating transformers and RC snubber networks used in the dual-bridge converter. Single-pole double-throw (SPDT) switches have been added to the transformer secondary with the SCR gate trigger for both bridge converters, so that only one converter can be triggered at any one time. The snubber circuits have been duplicated and connected in parallel with the additional SCRs.

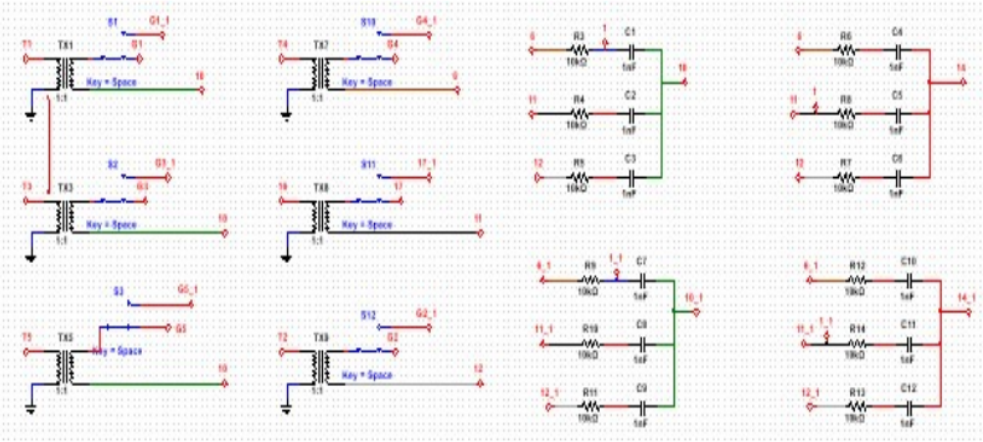
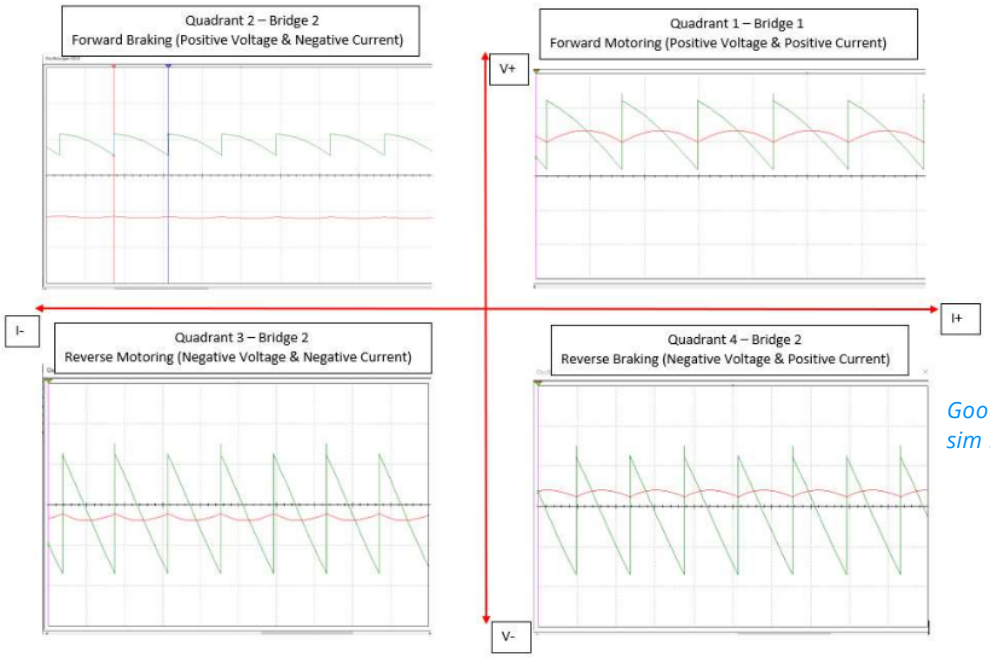


Figure 10 – Isolating Transformers and Snubber Networks of Design Adaption Circuit

Excellent work

4.2.1. 4-Quadrant Operation

Figure 11 displays the graphical results of all four quadrants from the Multisim simulation of the dual converter, which have been placed on a vertical voltage axis and a horizontal current axis to aid with the understanding of each quadrants operation. The green trace is voltage, while the red trace represents current.



Good annotated sim results

Figure 11 – Four Quadrant Operation with All Four Quadrants Displayed on Graph

Table 6 is a comparison table of the expected results from the research and actual simulation results of the four-quadrant operation. The simulated results, seen in figure 11, match with the expected result for each quadrant.

4-Quadrant Operation		
Quadrant	**Expected Result**	**Actual Simulated Result**
1	Forward Motoring (Positive Voltage & Current)	Forward Motoring (Positive Voltage & Current)
2	Forward Generating (Positive Voltage & Negative Current)	Forward Generating (Positive Voltage & Negative Current)
3	Reverse Motoring (Negative Voltage & Current)	Reverse Motoring (Negative Voltage & Current)
4	Reverse Generating (Negative Voltage & Positive Current)	Reverse Generating (Negative Voltage & Positive Current)

Table 6 – Four Quadrant Operation Expected Result Compared with Simulated Result

Excellent work here

5. Practical Investigations

5.1. Practical Task Setup

The practical setup for this assignment task is an AC and DC motor connected via a belt and pully system, seen in figure 12. The DC motor is controlled via a Siemens 3-phase Sinamics DCM converter (Part No.: 6RA8013-6DV62-0AA0). This drive can control the motor in all four quadrants. The AC motor is controlled via a Siemens S120 AC Variable Frequency Drive (VFD), which is setup to act as the load of the DC motor.

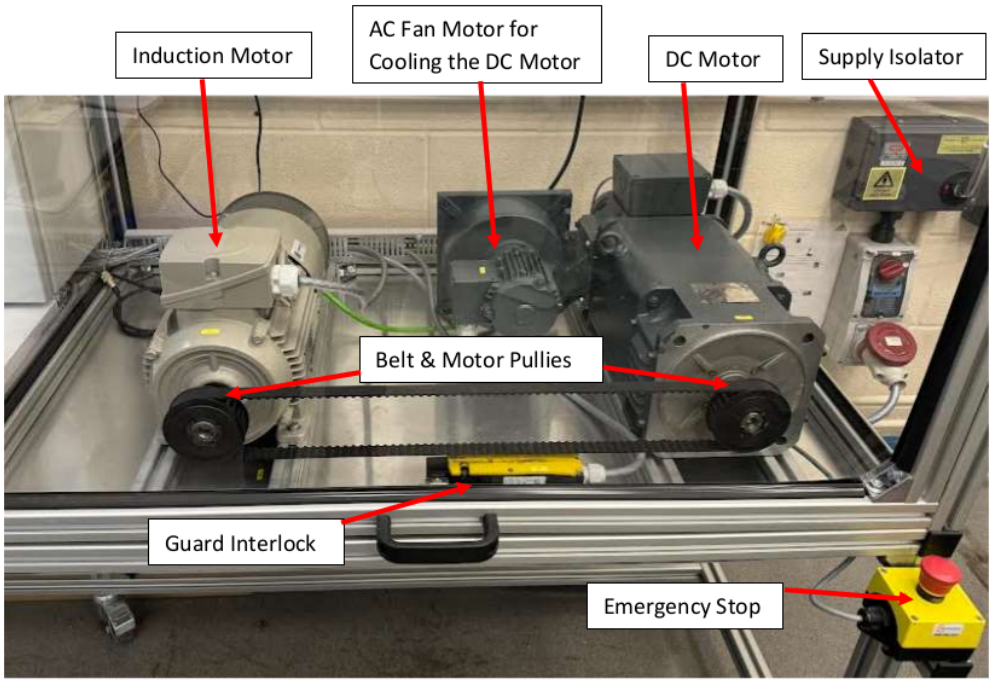


Figure 12 – AC-DC Motor System Setup with Annotations

The system is controlled via an S7-1511C Siemens fail-safe PLC and its associated TP1200 Comfort Panel HMI which allows operation of the motors through its interface. Part of the safety system can be seen in figure 12, with a guard interlock and emergency stop which will inhibit power to the motors. Figure 44 in appendix 8.3.1 shows the HMI and control panel for this system.

Good explanation and supporting diagram

Figure 13 shows a Fluke 325 True RMS Clamp Meter which was used for an additional test of the armature current which could be compared with the HMI and Picoscope values. The clamp is placed around the outgoing motor armature cable and the DC current will be displayed on the multi-meter. Figure 45 in section 8.3.1 of the appendix shows the Fluke and Picoscope clamp meters measuring the armature current. The Picoscope is set up to measure armature voltage and current, and line voltage and current. These values are then displayed on the Picoscope software.

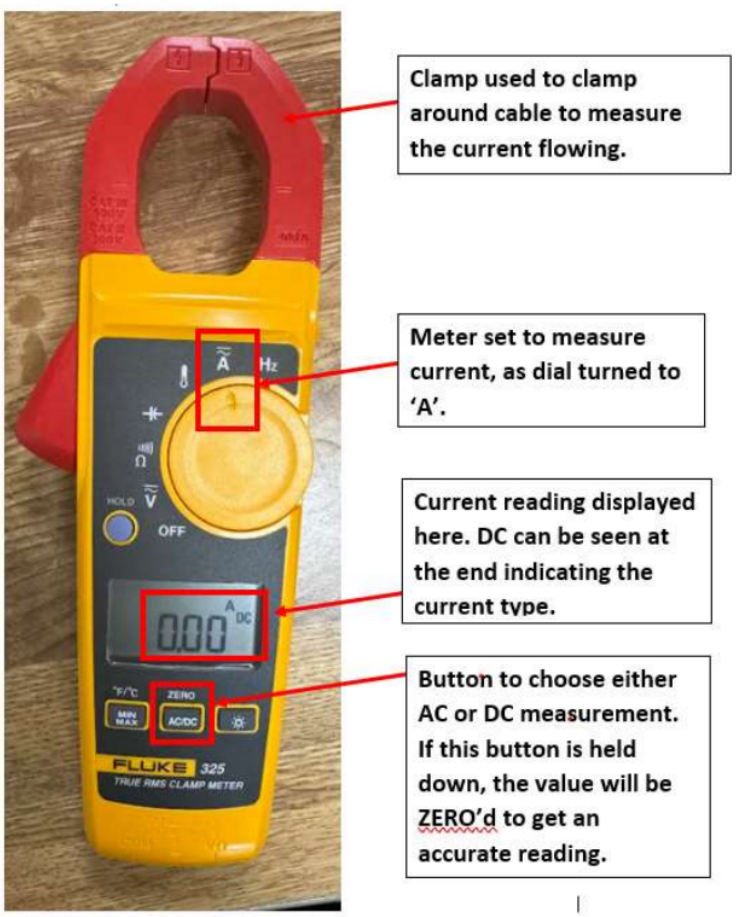


Figure 13 – Fluke 325 Clamp Meter with Annotations

Good detailed explanation and annotated diagram

5.2. 4-Quadrant Operation

Figure 14 shows the HMI control screen for running the motor in all 4 quadrants. The mode has been set to 'Auto' and 'Auto Start' has been pressed. A trace is set up to measure the speed, in blue, and the motor torque, in red. Each quadrant has been highlighted in green in figure 14.

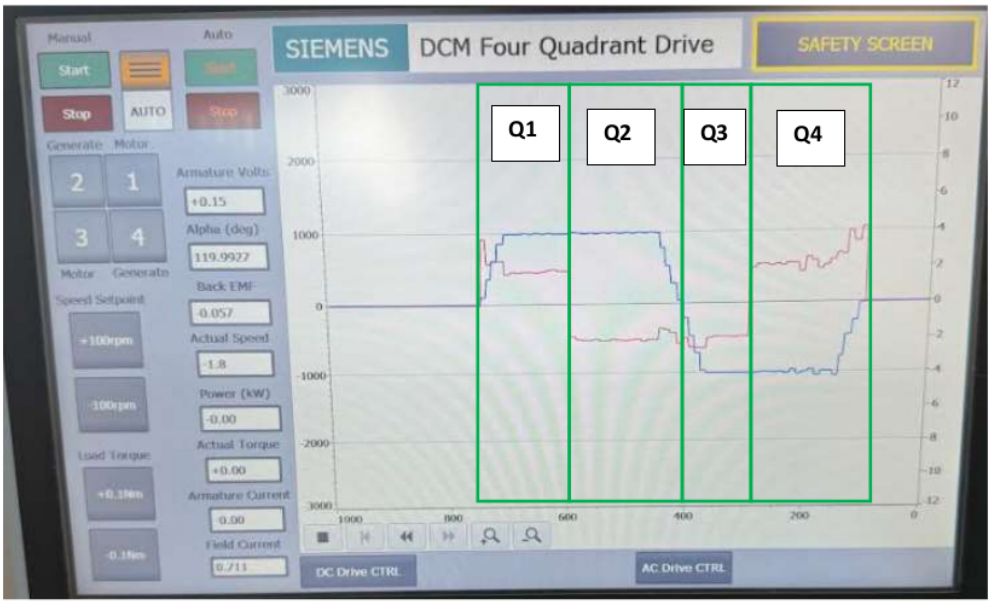
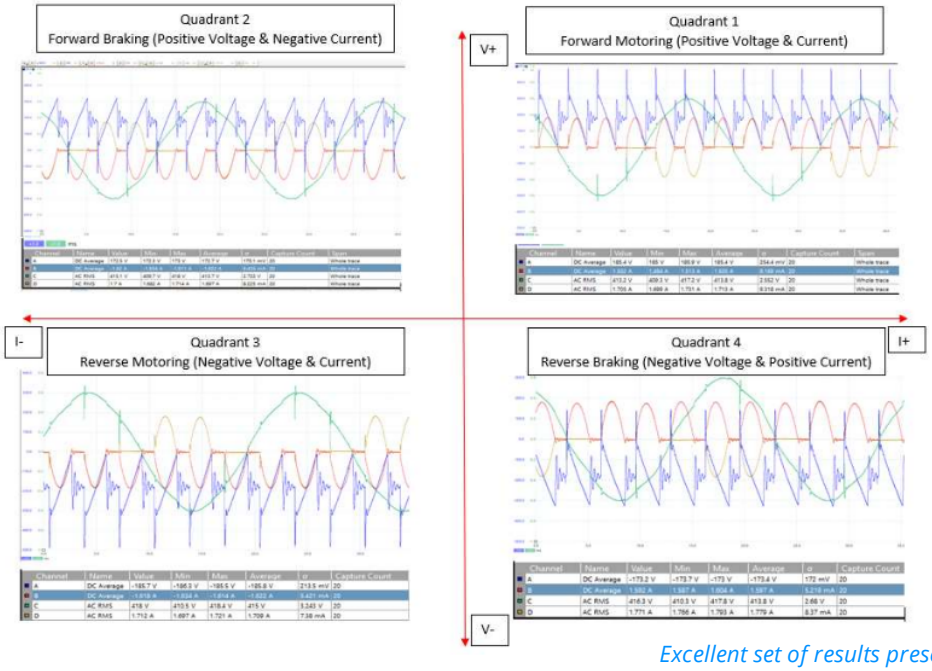


Figure 14 – Four Quadrant Operation on HMI Trace with Annotations

Excellent annotated results screenshot that identifies the 4 quadrant components orientation. This result agrees with the literature

Figure 15 displays the graphical results of all four quadrants from the Picoscope measurements of the dual converter, which have been placed on a vertical voltage axis and a horizontal current axis to aid with the understanding of each quadrants operation. See table 7 for the information regarding the trace.



Excellent set of results presented

Figure 15 – Four Quadrant Operation on Picoscope Displayed Graphically

Key	
Trace Colour	**Measurement**
Green	Line Voltage
Brown	Line Current
Blue	Armature Voltage
Red	Armature Current

Table 7 – Picoscope Key

Good use of table to identify key components on graphs

Table 8 is a comparison between the expected result of the speed and torque characteristics in 4-quadrant operation, with the HMI and Picoscope results. As the Picoscope is measuring the armature voltage and current, they will be used to represent speed and torque, respectively. As can be seen from table 8, this theory is proven correct as Picoscope results match the expected and HMI results.

4-QUADRANT OPERATION COMPARISON			
QUADRANT	**Expected**	**HMI**	**Picoscope**
1	Forward Motoring: Positive Speed & Positive Torque	Forward Motoring: Positive Speed & Positive Torque	Forward Motoring: Positive Voltage & Positive Torque
2	Forward Generating: Positive Speed & Negative Torque	Forward Generating: Positive Speed & Negative Torque	Forward Generating: Positive Voltage & Negative Torque
3	Reverse Motoring: Negative Speed & Negative Torque	Reverse Motoring: Negative Speed & Negative Torque	Reverse Motoring: Negative Voltage & Negative Torque
4	Reverse Generating: Negative Speed & Positive Torque	Reverse Generating: Negative Speed & Positive Torque	Reverse Generating: Negative Voltage & Positive Torque

Good table of comparison

Table 8 – Four Quadrant Operation Comparison Between Expected, HMI & Picoscope Results

Table 9 shows the motor parameters taken from the HMI for each of the 4 quadrants. The evidence of this can be seen in appendix 8.3.2.

FOUR QUADRANT OPERATION				
OPERATING PARAMETERS	**Q1**	**Q2**	**Q3**	**Q4**
ARMATURE VOLTAGE (VA)	185.83	173.09	-184.39	-172.93
ALPHA (DEGREES)	81.56	115.89	82.08	115.18
BACK EMF (V)	180.77	178.79	-181.12	-179.02
ACTUAL SPEED (RPM)	1002	997.5	-1001.5	-1008
POWER (KW)	0.29	-0.25	0.27	-0.28
ACTUAL TORQUE (NM)	1.94	-1.91	-1.93	2.07
ARMATURE CURRENT (IA)	1.5	-1.49	-1.47	1.57
FIELD CURRENT (IF)	18.69	18.68	18.68	18.69

Good set of results that follow the 4 quadrant operation procedure

Table 9 – Four Quadrant Operation HMI Drive Values

In quadrant 1, both armature voltage and current are positive indicating the motor is in forward motoring mode. This is supported by the fact the torque is positive, the back EMF is lower than the armature voltage and the firing angle is less than 90°.

In quadrant 2, armature voltage is positive, but armature current is negative, indicating the motor is in forward braking mode. This is supported by the fact the torque is negative, the back EMF is higher than the armature voltage and the firing angle is greater than 90°.

In quadrant 3, both armature voltage and current are negative indicating the motor is in reverse motoring mode. This is supported by the fact the torque is negative, the back EMF is a lower magnitude than the armature voltage and the firing angle is less than 90°.

In quadrant 4, armature voltage is negative, but armature current is positive, indicating the motor is in reverse braking mode. This is supported by the fact the torque is positive, the back EMF has a higher magnitude than the armature voltage and the firing angle is greater than 90°.

From these results, it can be concluded that current and torque are proportional, as well as speed and voltage. The field current remains constant throughout the 4 quadrants of operation. The current polarity also indicates which bridge is operating, with positive current indicting bridge 1 is in operation and negative current indicates bridge 2 is in operation.

Good explanation

Table 10 is a comparison between the armature voltage and current of the DC motor tested with three sets of test equipment, the drive values displayed on the HMI, the Fluke current clamp meter and the clamp meter for the Picoscope.

HMI, Clamp & Picoscope Armature Voltage & Current Comparison				
Quadrant	Test	Parameters		Figure
		Armature Voltage (Va)	Armature Current (Ia)	
Q1	HMI	185.83	1.5	46
	Picoscope	185.4	1.5	47
	Clamp		1.43	48
Q2	HMI	173.09	-1.49	49
	Picoscope	172.5	-1.62	50
	Clamp		-1.8	51
Q3	HMI	-184.39	-1.47	52
	Picoscope	-185.7	-1.62	53
	Clamp		-1.73	54
Q4	HMI	-172.93	1.57	55
	Picoscope	-173.2	1.59	56
	Clamp		1.53	57

Table 10 – Armature Voltage & Current Comparison Between HMI, Fluke Clamp & Picoscope

Excellent work here

5.3. Speed Setpoints with Constant Torque DC Motor Analysis

5.3.1. 1000RPM Test & Calculations

A test was undertaken to demonstrate discontinuous current by running the DC drive in quadrant 1 for three speed setpoints, while keeping torque constant. The motor parameters were taken and tabulated for each of the three speed setpoints and compared.

The three speed setpoints were 1000RPM, 1400RPM and 1800RPM. The HMI and Picoscope results for 1000RPM can be seen in figures 16 and 17. The remaining tests can be seen in appendix 8.3.3.

Good explanation

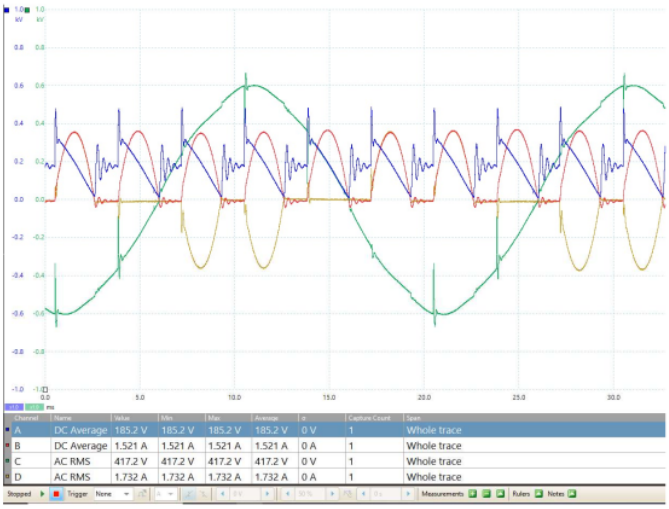


Figure 16 – 1000RPM Picoscope Graph

Good test result

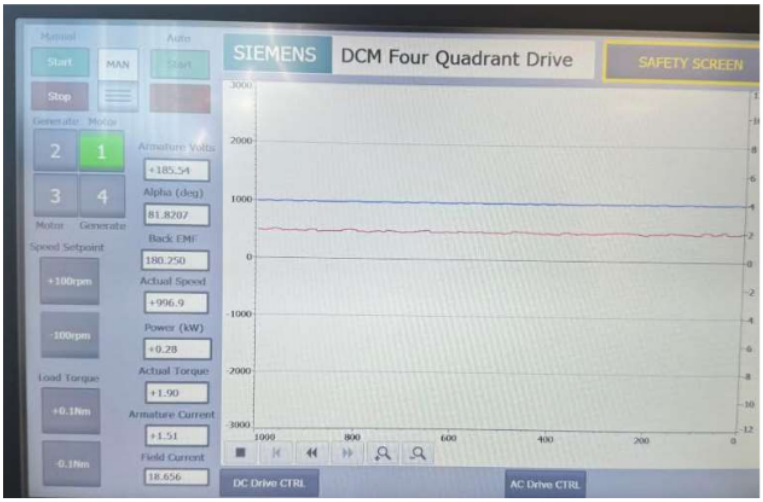


Figure 17 – 1000RPM HMI Result

Back EMF and firing angle values taken from the HMI in figure 17 were used to calculate the average armature voltage from the Picoscope waveform for the 1000RPM test. Vmax was found by measuring the input AC voltage with the Picoscope, this can be seen in figure 58 in appendix 8.3.3.

Table 11 shows the values to be used in the 1000RPM calculations.

Parameters	Value
E (Back EMF)	180.25V
α (Firing Angle)	81.82°
Vmax	591V

Table 11 – 1000RPM Calculation Values

Good table of results

These values can then be substituted into the following equations.

$$Area\ A = E\ \times\ \gamma = E\left(\alpha - \frac{\pi}{3}\right)$$

Equation 4 – Area A Calculation

$$Area\ B = Vmax \int_{\frac{\pi}{3}+\alpha}^{\pi} \sin(\theta)\, d\theta = Vmax[-cos\theta]\ \frac{\pi}{3} + \alpha^{\pi}$$

$$Area\ B = Vmax\left(-cos - -\cos\left(\frac{\pi}{3} + \alpha\right)\right) = Vmax\left(1 + \frac{1}{2}\cos(\alpha) - \frac{\sqrt{3}}{2}\sin(\alpha)\right)$$

Equation 5 – Area B Calculation

$$V_{mean} = \frac{Area\ A + Area\ B}{\pi/3}$$

Equation 6 – Vmean Calculation

To start, α must be converted into radians:

$$\alpha = 81.82\ \times \frac{\pi}{180} = 1.43$$

Equation 7 – $1000RPM\ \alpha\ Calculation$

Area A:

$$Area\ A = E\left(\alpha - \frac{\pi}{3}\right) = 180.25(1.43 - 1.047) = 69.04V$$

Equation 8 – 1000RPM Area A Calculation Result

Area B:

$$Area\ B = 591(1 + \frac{1}{2}\cos(1.43) - \frac{\sqrt{3}}{2}\sin(1.43)) = 125.71V$$

Equation 9 – 1000RPM Area B Calculation Result

V_{mean}:

$$V_{mean} = \frac{69.04 + 125.71}{\pi/3} = 185.97V$$

Good work

Equation 10 – Vmean Calculation Result

Discontinuous Current Speed Test				
Speed	**Picoscope Voltage**	**Calculated Voltage**	**Error**	
1000RPM	185.2V	185.97V	0.77V	0.41%
1400RPM	256.7V	234.7V	22V	8.95%
1800RPM	328V	279.98V	48.02V	15.8%

Table 12 – Discontinuous Current Speed Test

Table 12 shows a comparison between the Picoscope armature voltage and the calculated armature voltage for each speed setpoint. There is a minor error between the values for 1000RPM, which could be due to rounding errors in the calculations or the scaling of Picoscope measurement. But there are significant errors as the speed increases, as 1400RPM has a 22V error and 1800RPM has a 48.02V error. The calculations for the 1400RPM and 1800RPM tests can be seen in appendix 8.3.3.

Very good explanation and use of tables for results

5.3.2. Discontinuous Current Speed Setpoint Test Results

Table 13 shows the HMI results of the three speed setpoints. The 1400RPM and 1800RPM tests can be seen in appendix 8.3.3.

Good ref to appendix

Discontinuous Current: Three Speeds at Constant Torque						
Operating Parameters	**1000RPM**		**1400RPM**		**1800RPM**	
	HMI	**Picoscope**	**HMI**	**Picoscope**	**HMI**	**Picoscope**
Armature Voltage (Va)	185.54	185.2	257.02	256.7	330.47	328
Alpha (Degrees)	81.82		73.09		60.74	
Back EMF (V)	180.25		251.81		324.35	
Actual Speed (Rpm)	996.9		1402.6		1799.9	
Power (kW)	0.28		0.4		0.56	
Actual Torque (Nm)	1.9		1.95		1.73	
Armature Current (Ia)	1.51	1.52	1.6	1.57	1.36	1.54
Field Current (If)	18.66		18.68		18.67	

Good table of values for comparison

Table 13 – Discontinuous Current Speed Test Results

The voltage increases linearly with an increase in RPM, proving the relationship between speed and armature voltage. The increase of RPM also shows a decrease of the 'Alpha' firing angle, which supports the theories researched, as more of the wave is processed – therefore increasing the voltage applied to the motor. The back EMF increases with speed, as armature voltage increases, but remains lower around 5-6V lower than the armature voltage. Power increases with the speed, as expected due to the increase in voltage.

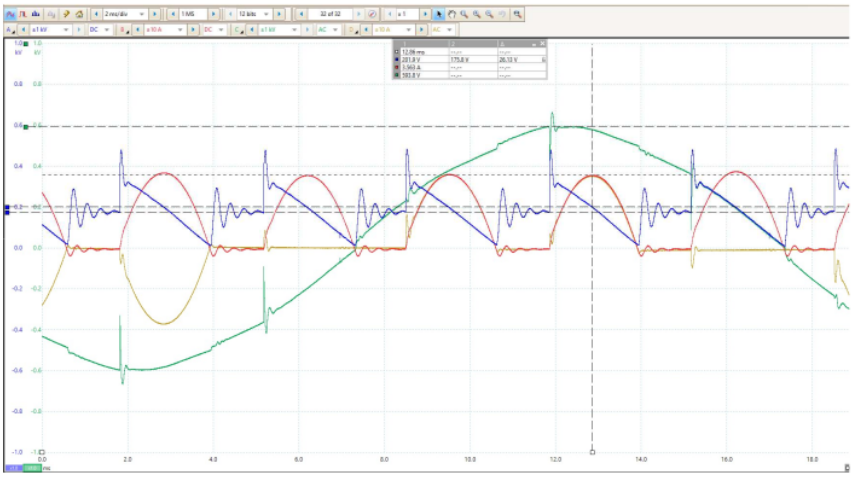
Good explanation

The torque remains constant throughout the testing, apart from a slight drop in the HMI value at 1800RPM, which could be due to when the snapshot of the HMI values was taken. As current is proportional to torque, current also remains constant apart from the HMI value at 1800RPM, like the torque, but the Picoscope current remains constant at around 1.5A within a 0.05A range.

Very good argument that agrees with theory

5.3.3. DC Motor Constants

Figure 18 shows the Picoscope graph with cursors to measure Va, back EMF and current.



Channel	Name	Value	Min	Max	Average	σ	Capture Count	Span
A	DC Average	185.7 V	185.7 V	185.7 V	185.7 V	0 V	1	Whole trace
B	DC Average	1.521 A	1.521 A	1.521 A	1.521 A	0 A	1	Whole trace
C	AC RMS	413 V	413 V	413 V	413 V	0 V	1	Whole trace
D	AC RMS	1.732 A	1.732 A	1.732 A	1.732 A	0 A	1	Whole trace

Figure 18 – Picoscope DC Motor Constant Values

Figure 19 displays a close-up of the Picoscope cursor values.

1	2	Δ
12.86 ms	--.--	--.--
201.9 V	175.8 V	26.13 V
3.563 A	--.--	--.--
593.8 V	--.--	--.--

Figure 19 – Picoscope Cursor Values

Good test results with values needed for calculations

From figure 19:

Va = 201.9V

EMF = 175.8V

The values are used in equation 8 to calculate dynamic resistance:

$$Va = E + IaRa + L\frac{di}{dt}$$

Equation 11 – Armature Voltage Calculation

Formula is identified

$$At\ Peak\ Current, L\frac{di}{dt} = 0$$

The equation can then be rearranged for armature resistance:

$$Ra = \frac{(Va - E)}{Ia} = \frac{26.13}{3.563} = 7.33\Omega$$

Good work

Equation 12 – Armature Resistance Calculation

The armature resistance value can then be confirmed by substituting the value into equation 11 to find VA:

$$Va = 175.8 + (3.563 \times 7.33) = 201.9V$$

Formula check proves result for Ra

Equation 13 – Armature Voltage Calculation Result

To find further motor constants, values were taken from the HMI with the motor running in quadrant 1 at 1000RPM, seen in figure 20.

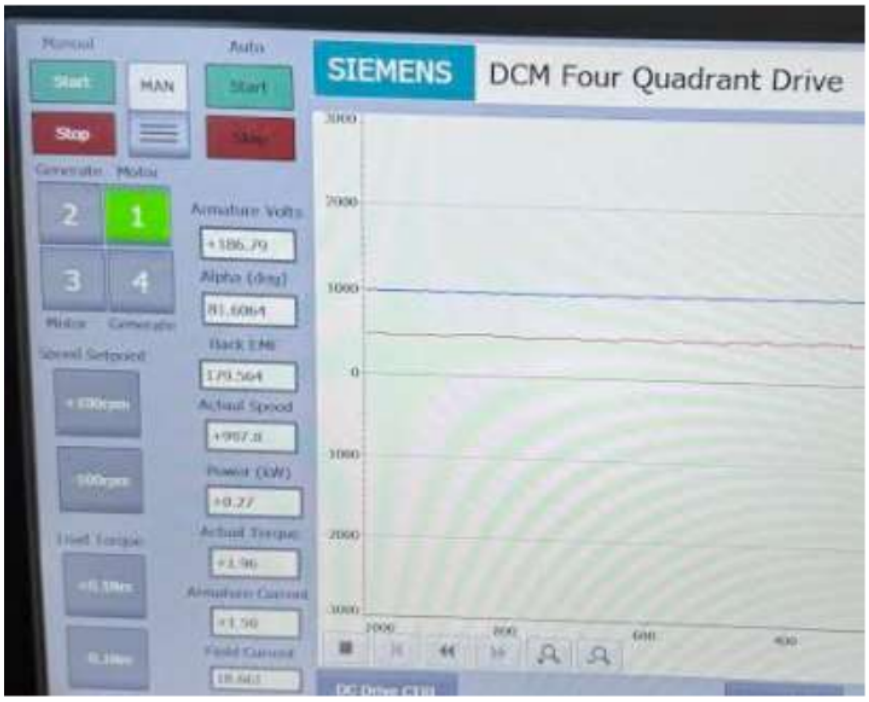


Figure 20 – HMI DC Motor Constant Values

The DC motor torque constant can be calculated using equation 14:

$$Kt = \frac{T}{Ia} = \frac{1.96}{1.5} = 1.31Nm/A$$

Good work

Equation 14 – DC Motor Torque Constant

The back EMF constant can be calculated using equation 12:

$$Ke = \frac{Ea}{\omega}$$

Equation 15 – Back EMF Constant

Where ω equates to:

$$\omega = \frac{RPM}{2\pi} = \frac{997.8}{2\pi} = 158.8$$

$$\therefore Ke = \frac{Ea}{\omega} = \frac{179.56}{158.8} = 1.13V\ /Krpm$$

Good work

Equation 16 – Ke Constant

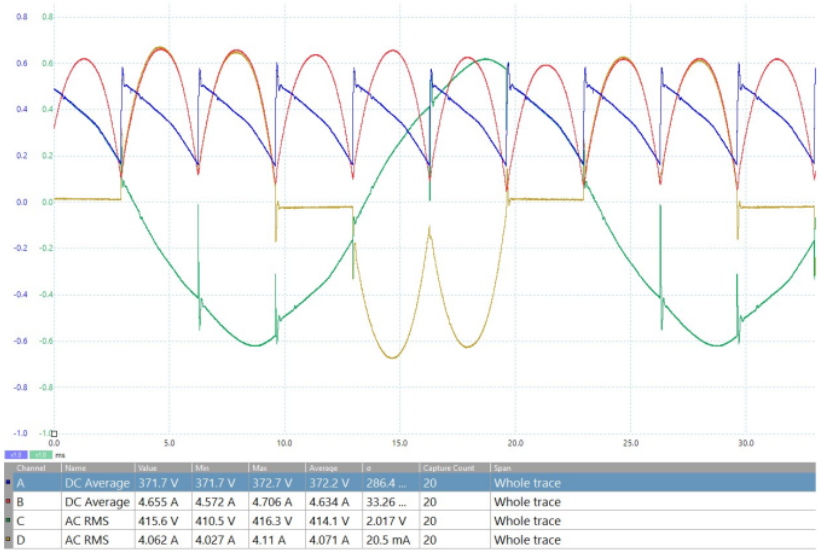
Good work here. Formula has been identified and used to find constants related to the motor.

5.4. Continuous Current Torque Setpoints DC Motor Analysis

A test was undertaken to demonstrate continuous current by running the DC drive in quadrant 1 for three torque setpoints, while keeping speed constant. The motor parameters were taken and tabulated for each of the three torque setpoints and compared.

The three torque setpoints were 6Nm, 4.5Nm and 3Nm. The Picoscope and HMI results for 6Nm can be seen in figures 21 and 22. The remaining tests can be seen in appendix 8.3.4.

Good explanation of procedure and test result for continuous current



Channel	Name	Value	Min	Max	Average	σ	Capture Count	Span
A	DC Average	371.7 V	371.7 V	372.7 V	372.2 V	286.4 ...	20	Whole trace
B	DC Average	4.655 A	4.572 A	4.706 A	4.634 A	33.26 ...	20	Whole trace
C	AC RMS	415.6 V	410.5 V	416.3 V	414.1 V	2.017 V	20	Whole trace
D	AC RMS	4.062 A	4.027 A	4.11 A	4.071 A	20.5 mA	20	Whole trace

Figure 21 – Picoscope Result at 6Nm

Good values obtained

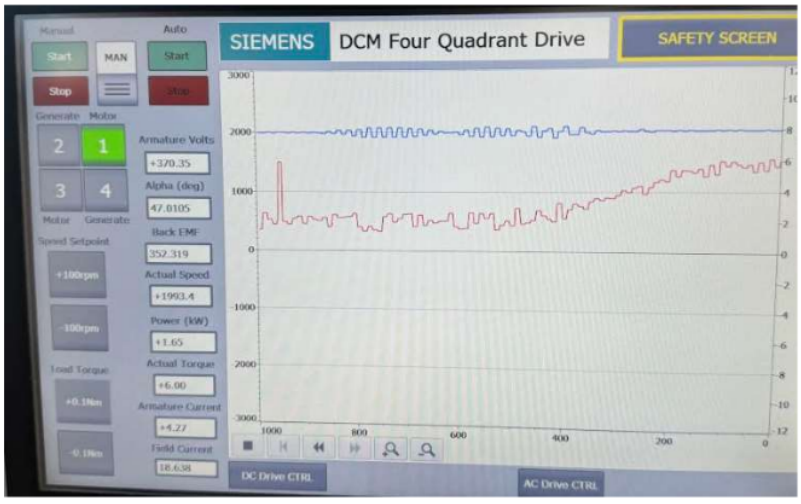


Figure 22 – HMI Result at 6Nm

The motor parameters were taken from the Picoscope, and the DC drive values displayed on the HMI for the variable torque tests and tabulated in table 14. The speed was kept constant at 2000RPM, and the current was continuous.

Continuous Current: Three Torque Setpoints at Constant Speed						
Operating Parameters	**6Nm**		**4.5Nm**		**3Nm**	
	HMI	**Picoscope**	**HMI**	**Picoscope**	**HMI**	**Picoscope**
Armature Voltage (Va)	370.35	371.7	368.04	370.3	371.16	366.1
Alpha (Degrees)	47.01		47.77		50.16	
Back EMF (V)	352.32		358.9		359.41	
Actual Speed (Rpm)	1993.4		2005.5		1980.8	
Power (kW)	1.65		1.27		0.9	
Actual Torque (Nm)	6		4.51		2.98	
Armature Current (Ia)	4.27	4.66	3.24	3.58	2.11	2.36
Field Current (If)	18.64		18.65		18.67	

Table 14 – Continuous Current Torque Setpoint Results

Excellent work

From table 14, the relationship between armature voltage and speed can be seen again, as the speed was kept at around 2000RPM due to the requirements of the tests and voltage also remained constant, at around 370V. The firing angle also remains constant at 47°- 50°, as does the back EMF which would be expected as the voltage remains constant.

Current can be seen to be proportional to torque, as when one decreases so does the other. The power also decreases over the three tests due to the lower current of the motor. There is a slight discrepancy in the HMI and Picoscope values for armature current, with the errors ranging from 0.25 – 0.39. The error between the current values decreases as the current decreases, which could be due to an issue with the scaling of the Picoscope set up when the current is at higher values.

Acceptable errors

Very good explanation that includes significant points

6. Conclusions and Recommendations

In conclusion, this assignment has been successful in regard to the research, simulation, practical testing and investigation into DC drives and their control methods.

Research was conducted on advanced power electronic circuits, electrical machines, and drive systems and their associated applications, with the theory learnt from these topics then applied to the simulation and practical tasks in this assignment. A portion of the research section was spent on the design features and control techniques used in a three-phase, four quadrant DC drive, with the speed feedback and armature current feedback of the speed control loop investigated. *Good points included*

An in-depth look into the specification of a Parker 590+ Series DC drive was conducted, were areas such as the minimum requirements to operate this drive were understood, with only an enable, run, emergency stop, and speed reference signal required to run this drive in its most rudimentary form. The operating specification was also detailed, with such characteristics as incoming voltage and current, outgoing voltage, power and current, operating speeds and its four-quadrant operation. *Good significant points form research findings*

The last section of research that was undertaken was specifying the typical applications of four quadrant DC motors and their comparisons with AC drives. In the past, the DC motor and drive were the workhorse of industry but with advancements to AC motors and drives, the need for their DC equivalents is reducing. But there were certain applications, most which require motors to run at low speeds, where the DC motor and drive is superior to the AC counterpart – such as cranes and hoists which require a load to be raised and lowered at low speeds. The accuracy of a DC drive at low speeds and its ability to control torque is superior to other drive options. *Good valid points covered here*

This is a good valid point

Once the research was complete, a simulation using NI Multisim was created to model a separately excited DC motor controlled via a three-phase fully-controlled full-wave rectifier. This drive was modelled by utilising a phase-angle controller, which mimicked the firing angle control of a drive, which triggered the gates of the SCRs used. The simulation showed that as the firing angle increased, the armature voltage decreased and as such, the speed decreased. This was the expected result from the theory and proved the validity of the research that was conducted. Tests were conducted to find the armature voltage when altering the firing angle, and the simulated values were compared with calculated values. There were negligible errors between the simulated and calculated results, with the biggest error being 0.27V, proving that the simulation model is highly effective.

Good points included

Purpose of adapted drive to accomodate 4 quadrant operation

The original simulation design was then adapted to operate in all four-quadrants by inserting a second SCR bridge in anti-parallel to the load, which allowed operation in quadrants 2 and 3. An oscilloscope was utilised in the simulation to measure the armature voltage and current in each quadrant and these results were then compared with the expected results from the theory, with the correct waveforms produced for each quadrant – proving the adaption was successful.

During the practical investigation, the Siemens DC drive underwent operation in all four quadrants, employing the Siemens AC motor as a load. Performance data was systematically gathered from each quadrant, utilising tools such as the HMI trace graph, Picoscope waveforms, and a Fluke 325 current clamp meter. The collected results were tabulated, facilitating a thorough comparison. Notably, the three testing instruments demonstrated accuracy, aligning closely with the anticipated outcomes based on theoretical expectations. The investigation successfully validated the proportional relationship between armature voltage and speed, as well as the proportional connection between torque and current. *Good valid points*

Two additional practical tests were conducted, one involving speed variations and the other focusing on torque adjustments. The motor speed test effectively validated the correlation between armature voltage and speed, providing support for this relationship. Similarly, the torque test demonstrated the connection between torque and current, serving as the second method to affirm the theoretical framework for both relationships. This cohesive result reinforces the accuracy of the theory, simulation, and practical experiments, collectively validating the established relationships between armature voltage and speed, and motor current and torque. *Good points covered*

The addition of an extra piece of test equipment, the Fluke 325 current clamp meter, for the practical task proved successful with the results matching the HMI and Picoscope values – improving the reliability of results for this assignment. A recommendation to improve this assignment would be the addition of this test equipment to all future assignments, so future students will gain a third set of results for comparison. The Fluke meter could also be used to measure voltage, if it could be set up to safely measure the required points with clips placed on the terminals. *Good recommendation*

A second recommendation would be to include the actual set up of the AC and DC drives to the assignment, with options such as performing a no-load ‘auto-tune’ for both drives which would first require inputting the motor constants from the motor nameplate into the drive, with values such as base speed, number of poles, power factor, and frequency for an AC motor. The ‘auto-tune’ would then calculate other motor parameters and save them in the drive, and set various gains in order to run the motor properly. *A very good recommendation*

7. References

Circuit Globe, 2017. *Four Quadrant Operation of DC Motor.* [Online]
Available at: https://circuitglobe.com/four-quadrant-operation-of-dc-motor.html
[Accessed 02 02 2024].

Drury, B., 2001. *The Control Techniques Drives & Controls Handbook.* 1st ed. Cambridge: Cambridge University Press.

Hughes, A., 2009. *Electric Motors & Drives.* 3rd ed. Oxford: Newnes.

Invertek Drives , 2024. *Cranes, Hoists & Elevators.* [Online]
Available at: https://www.invertekdrives.com/support/iknow/selection-and-installation/cranes-hoists-and-elevators-17#:~:text=This%20means%20the%20drive%20has,only%20operate%20in%20two%20quadrants.
[Accessed 03 02 2024].

Krishnan, R., 2001. *Electric motor drives : modeling, analysis, and control.* Upper Saddle River, NJ: Prentice-Hall.

Lander, C., 1993. *Power Electronics.* 3rd ed. Maidenhead: McGraw-Hill.

MathWorks, 2024. *Field Weakening Control.* [Online]
Available at: https://uk.mathworks.com/discovery/field-weakening-control.html
[Accessed 02 02 2024].

Mohan, N. & Undeland, T., 2003. *Power electronics : converters, applications and design.* 3rd ed. Chichester: Wiley.

Parker, 2024. *590+ Series Digital DC Drives Manual.* [Online]
Available at: https://www.parker.com/content/dam/Parker-com/Literature/SSD-Drives/DC-Drives/HA466461U004.pdf
[Accessed 01 02 2024].

Rashid, M. H., 2013. *Power electronics: devices, circuits, and applications.* International edition ed. s.l.:Pearson Education.

Rashid, M. H., 2014. *Power Electronics: Devices, Circuits & Applications.* 4th ed. Harlow: Pearson.

Weidauer, J. & Messer, R., 2014. *Electric Drives.* 1st ed. Berlin: Publicis.

Wilamowski, B. & Irwin, J. D., 2017. *Power Electronics and Motor Drives.* 2nd ed. Boca Raton, FL: CRC Press.

Wildi, T., 2014. *Electrical machines, drives, and power systems.* 6th ed. Harlow: Pearson.

Good number of ref sources

8. Appendix

8.1. Appendix for Section 3

8.1.1. Design Features & Control Techniques Supporting Evidence

There are two different speed control loops that can control the speed of the motor, the armature voltage loop and the field flux control loop. The armature voltage loop is used for controlling the speed of the motor at or below base speed, with the field flux remaining constant in the armature voltage control loop. If the rated voltage is applied to the armature, the motor will run at its base speed. To lower the motor below base speed, the speed control loop increases the firing angle of the thyristors in the rectifier, which in turn, reduces the voltage applied to the armature (Drury, 2001). *Good point*

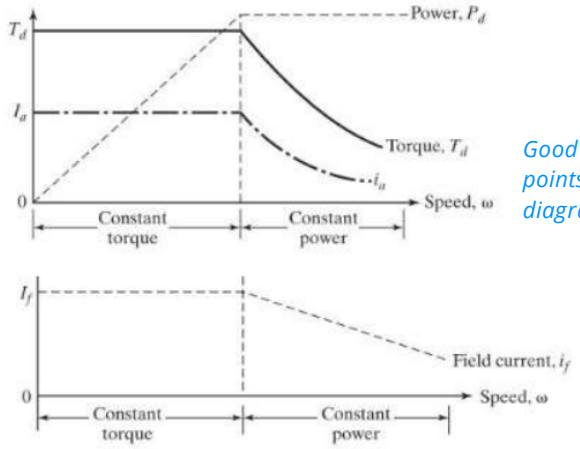
Good significant point here

To run the motor above base speed, the field flux control loop must be used. The rated armature voltage must be applied to the motor and then the field flux control begins to lower the field current, also called field weakening, which reduces the flux in the motor. This reduces the amount of back EMF, and as such this increases the armature current, increasing the speed of the motor (Weidauer & Messer, 2014). This is because speed is inversely proportional to field flux, and as field flux is proportional to field current, this means that if the field current is reduced then the flux will reduce – increasing the motor speed. This works by reducing the strength of the magnetic field, which in turn, reduces the back EMF in the armature – increasing the armature current and therefore, motor speed (Hughes, 2009).

Good point

Good explanation with relevant ref source

Figure 23 shows a speed graph of a DC motor and its power, torque and current characteristics up to and above base speed. Up to base speed, the torque, armature current and field current are constant, with armature voltage, power and speed increasing. Above base speed, field current decreases along with torque, thus increasing speed, while power remains constant.



Good explanations with significant points made and good supporting diagrams

Figure 23 – Torque & Power Characteristics Up to & Above Base Speed (Rashid, 2013)

Figure 24 shows a field weakening control loop of a DC drive. The armature current (Ia) is first fed into a filter and into the armature resistance (Ra) block, a signal is then sent from this block into a comparator with armature voltage (Va). This creates the back EMF signal ($Eg = Va - RaIa$) which is compared with the back EMF reference (EgRef), and the field controller then can reduce the field current to increase the motor speed.

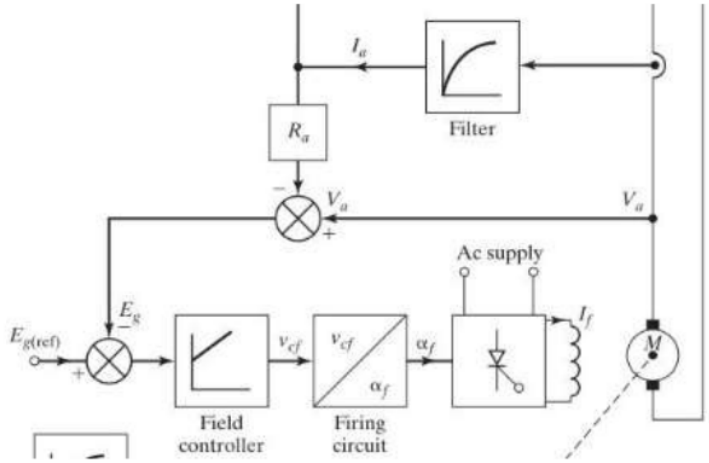
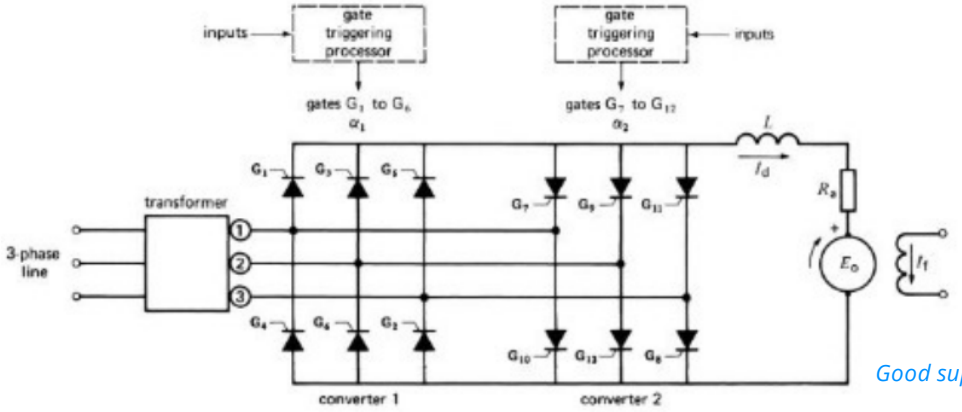


Figure 24 – Field Weakening Control Loop (Rashid, 2013)

Dual-converter thyristor drive, modified to allow four-quadrant operation. The second thyristor bridge, converter 2, has been added in anti-parallel to the load which will now allow operation in quadrants 2 and 3. This set up will be used in the design adaption in section 4.2.

Good explanation and supporting image



Good supporting image

Figure 25 – Dual Converter DC Drive (Rashid, 2013)

8.1.2. DC Drive Specification

Figure 26 shows the current loop of the Parker 590+ DC drive, with a signal from the speed loop, highlighted in green, that was detailed in figure 6 in section 3.2. The armature current feedback can also be seen, highlighted in blue, feeding into the comparator which sends a signal to the phase angle control, highlighted in red, which will control the required firing angle of the thyristors.

Good explanation and diagram

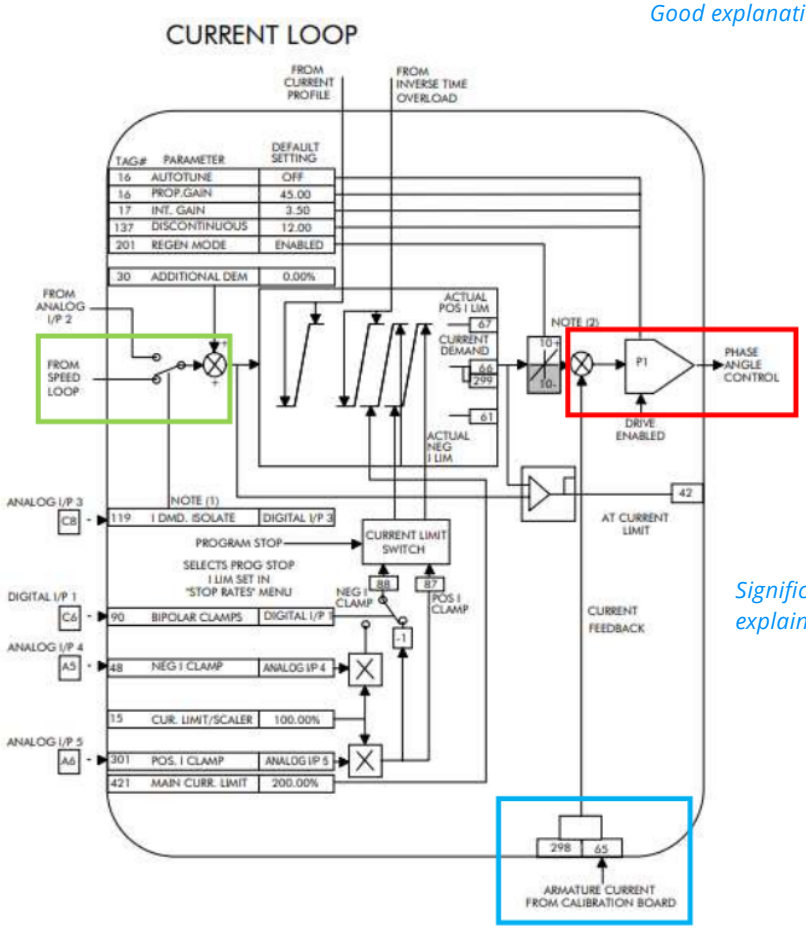


Figure 26 – Current Control Loop of Parker 590+ DC Drive (Parker, 2024)

Significant points ar highlighted and explained

Figure 27 shows the electrical schematic wiring of a Parker 590+ DC drive, including the power wiring and the control wiring.

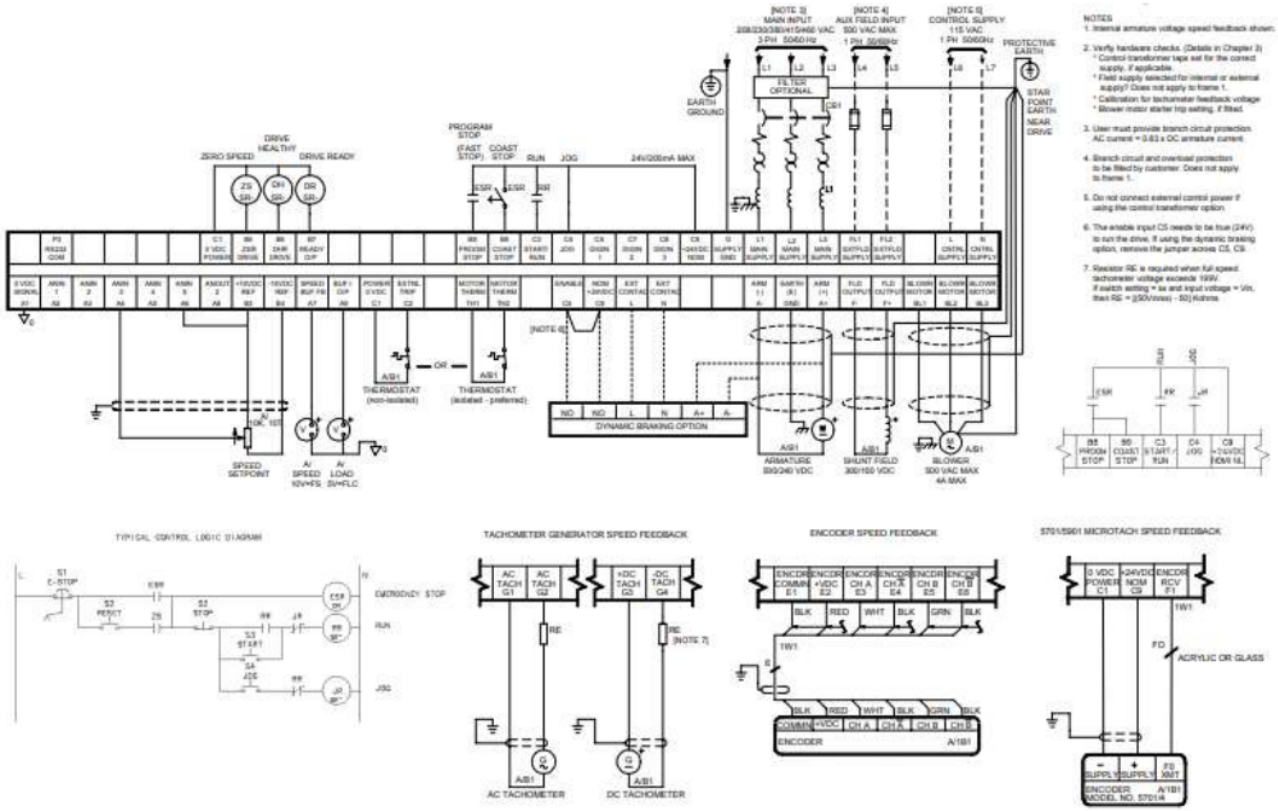


Figure 27 – Electrical Schematic of Parker 590+ DC Drive (Parker, 2024)

Figure 28 shows the physical arrangement of the Parker 590+ DC drive. Table 15 provides a key to describes the labelled parts of figure 28.

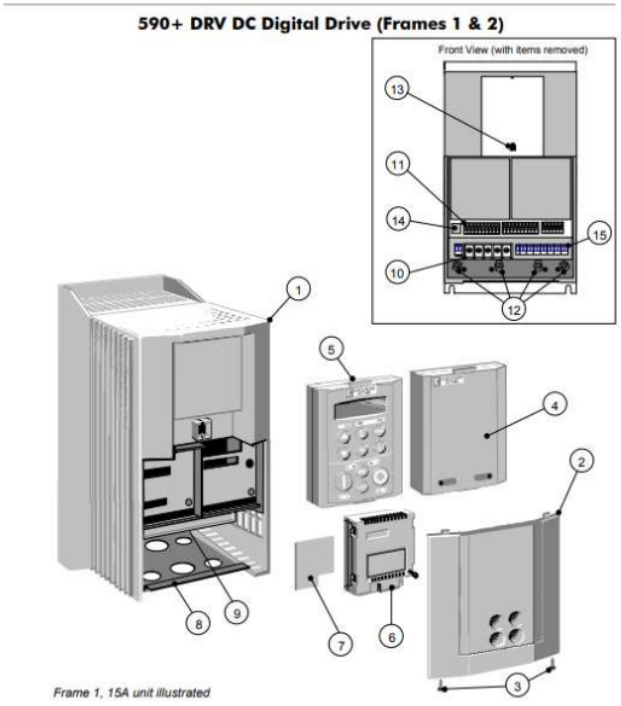


Figure 28 – Parker 590+ Labelled Description of Unit (Parker, 2024)

KEY	DESCRIPTION
1	Main Drive Assembly
2	Terminal Cover
3	Terminal Cover Retaining Screws
4	Blank Cover
5	6901 Keypad
6	COMMS Technology Box (Optional)
7	Speed Feedback Technology Card (Optional)
8	Gland Plate
9	Power Terminal Shield
10	Power Terminals
11	Control Terminals
12	Earthing/Grounding Points
13	Keypad Port
14	RS232 Programming Port
15	Auxiliary Power, External Contactor & Thermistor Terminals

Table 15 – Figure 28 Key

Key features of drive are identified

Figure 29 shows the field weakening control loop for the Parker 590+ DC drive. The field weakening PID controller, in green, is feeding into the field current PI controller, in blue, which then feeds the field thyristor firing control, which is in red.

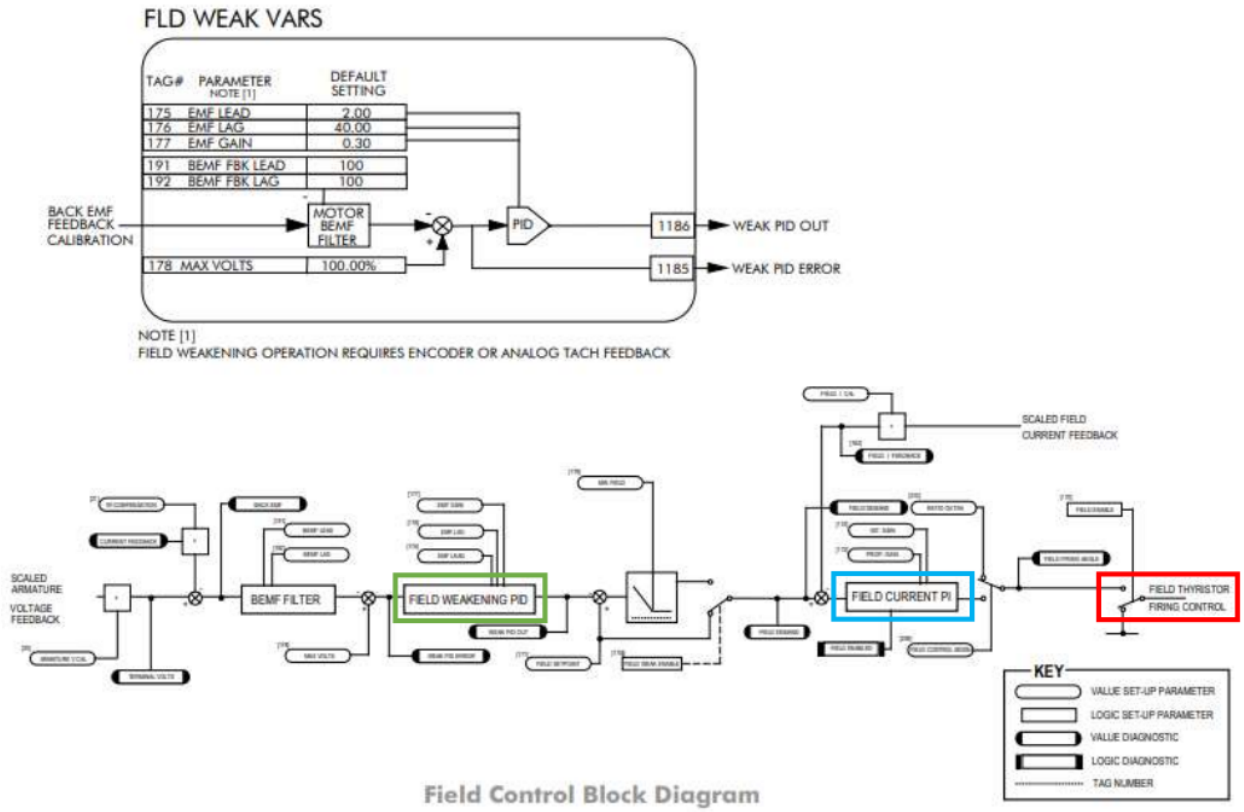


Figure 29 – Parker 590+ Field Weakening Control Loop (Parker, 2024)

Good supporting research with very good level of detail

8.1.3. Applications of 4-Quadrant DC Drives

An application for a 4-quadrat DC drive would be for an elevator, as the elevator must go up and down with and without a load, while also having a counterweight. To lift the passengers, the drive would be in quadrant 1, which would be motoring forwards, as a load would have to be lifted. But to drop the passengers, the drive would not run in quadrant 3, motoring reverse, because the added weight of the load could cause the elevator to descend to rapidly.

As such, the drive must operate in quadrant 4, reverse braking, so that the load is lowered in a safe and controlled manner. The same logic must be used for lifting the elevator without a load, as the load could be lifted rapidly. Due to this, the empty elevator is lifted via forward braking. The logic discussed above can be seen in figure 30.

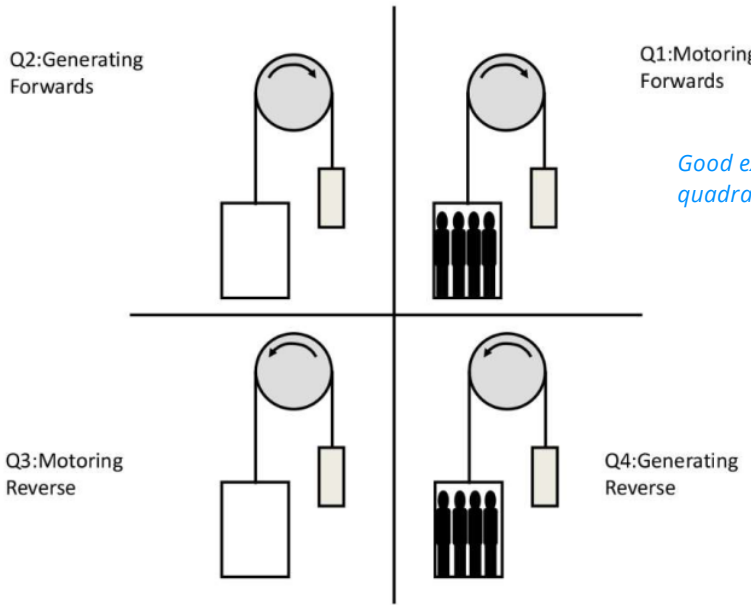


Figure 30 – 4-Quadrant Operation of an Elevator (Invertek Drives , 2024)

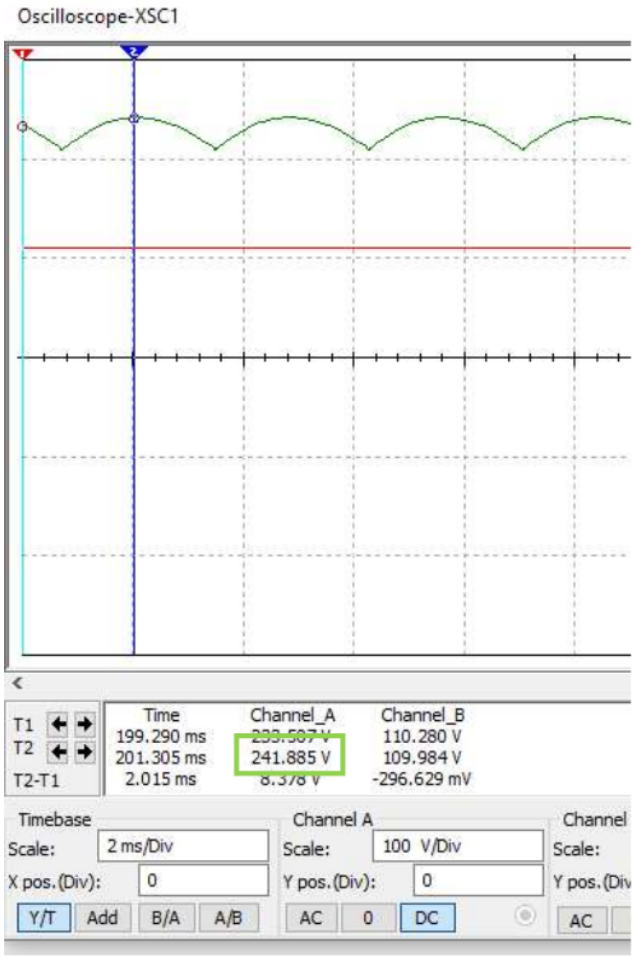
Good example that identifies the need for 4 quadrant operation

8.2. Appendix for Section 4

8.2.1. Three Phase Full Wave Controlled Rectifier Supporting Evidence

Firing Angle set to 0° & Vmax Displayed

Figure 31 displays the voltage and current waveforms when the firing angle is set to 0°. Vmax can be seen to be 242V via the blue cursor and highlighted via a green box.



Good test result

Figure 31 – Firing Angle set to 0°

Back EMF Polarity Reversed

Figure 32 shows the back EMF polarity reversed and the firing angle set to 90°, with both highlighted via a green box.

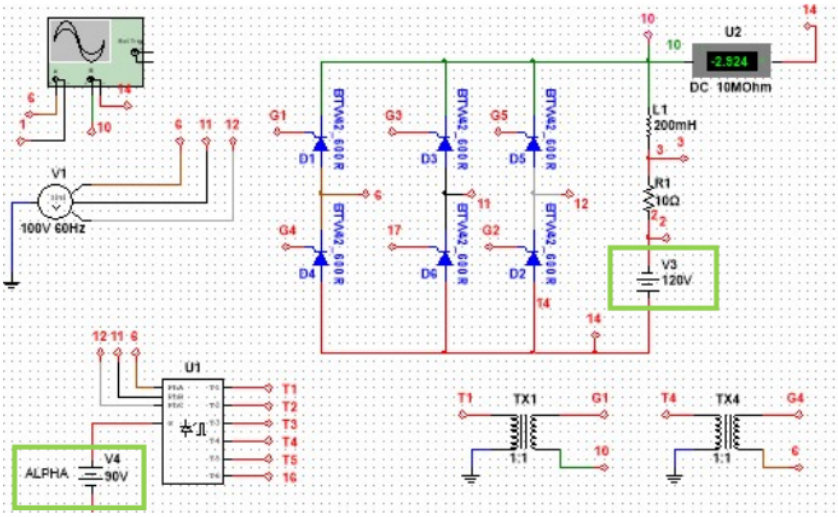
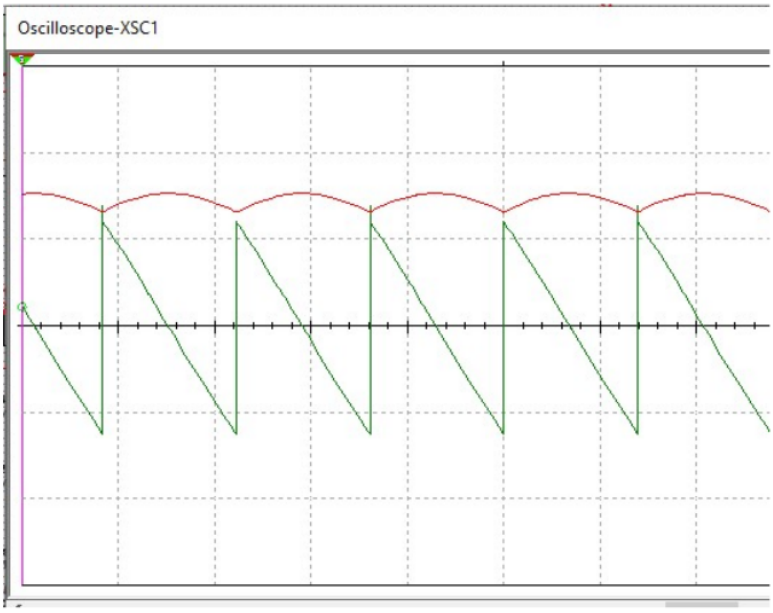


Figure 32 – Back EMF Polarity Reversed with Firing Angle set to 90°

Figure 33 shows the quadrant 4 oscilloscope trace, with current remaining positive and voltage going negative.



Good test that identifies quadrant 4 opertion for ths single converter drive

Figure 33 – Single Converter with Quadrant 4 Operation

Test 2 – 20° Firing Angle

Figure 34 shows the result of the 20° firing angle test, with the voltmeter value of 217V highlighted in blue. The oscilloscope waveform trace of the voltage and current can also been seen, with continuous current.

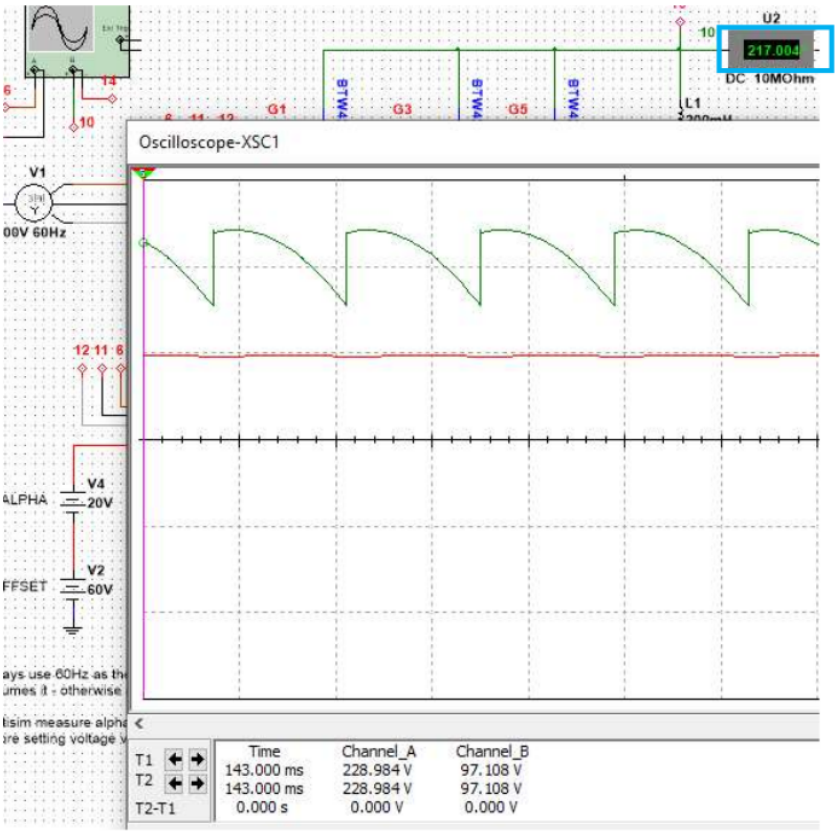


Figure 34 – Firing Angle set to 20°

Equation 2 can then be used to find the calculated value of the armature voltage. With Vmax = 242V and $\alpha = 20°$, substituted into equation 17.

Good test result

$$V_{mean} = \frac{3 \times 242}{\pi} \times Cos(20) = 217.16V$$

Equation 17 – Vmean Result at 20°

Test 3 – 30° Firing Angle

Figure 35 shows the result of the 30° firing angle test, with the voltmeter value of 199.9V highlighted in blue. The oscilloscope waveform trace of the voltage and current can also been seen, with continuous current.

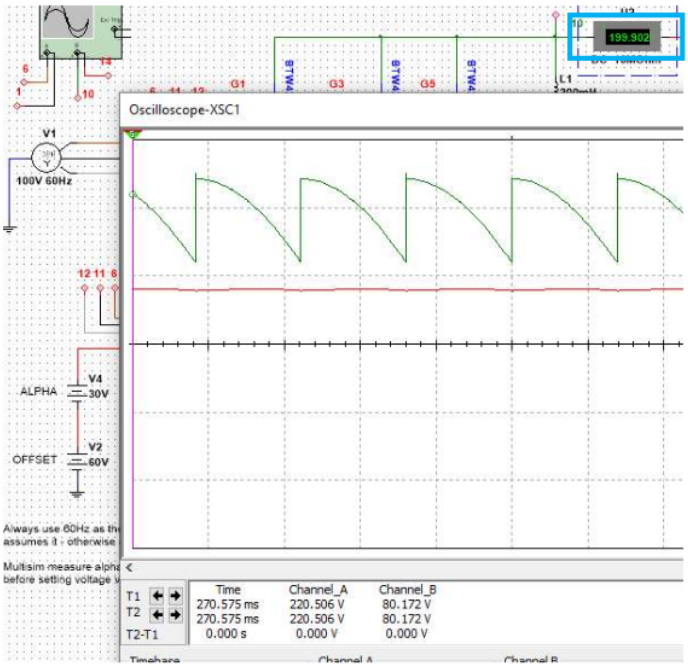


Figure 35 – Firing Angle set to 30°

Equation 2 can then be used to find the calculated value of the armature voltage. With Vmax = 242V and $\alpha = 30°$, substituted into equation 18.

$$V_{mean} = \frac{3 \times 242}{\pi} \times Cos(30) = 200.13V$$

Good test result

Equation 18 = Vmean Result at 30°

Test 4 – 40° Firing Angle

Figure 36 shows the result of the 40° firing angle test, with the voltmeter value of 176.76V highlighted in blue. The oscilloscope waveform trace of the voltage and current can also been seen, with continuous current.

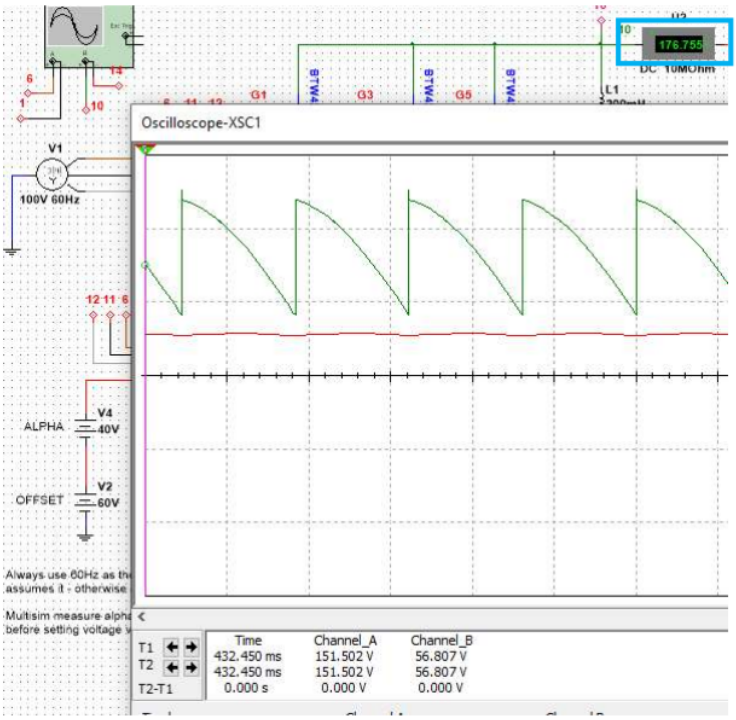


Figure 36 – Firing Angle set to 40°

Equation 2 can then be used to find the calculated value of the armature voltage. With Vmax = 242V and $\alpha = 40°$, substituted into equation 19.

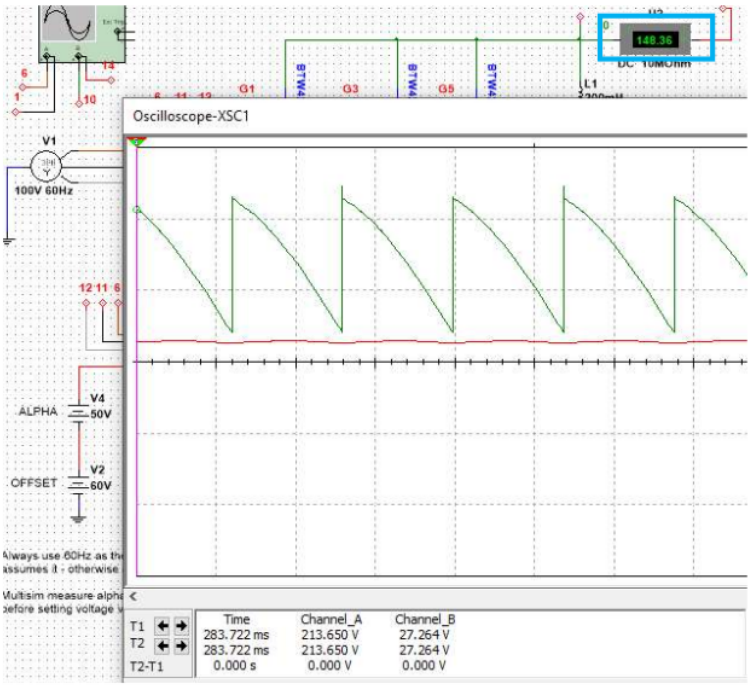
Good test result

$$V_{mean} = \frac{3 \times 242}{\pi} \times Cos(40) = 177.03V$$

Equation 19 – Vmean Result at 40°

Test 5 – 50° Firing Angle

Figure 37 shows the result of the 50° firing angle test, with the voltmeter value of 148.36V highlighted in blue. The oscilloscope waveform trace of the voltage and current can also been seen, with continuous current.



Good test result

Figure 37 – Firing Angle set to 50°

Equation 2 can then be used to find the calculated value of the armature voltage. With Vmax = 242V and $\alpha = 50°$, substituted into equation 20.

$$V_{mean} = \frac{3 \times 242}{\pi} \times Cos(50) = 148.54V$$

Equation 20 – Vmean Result at 50°

8.2.2. Design Adaption Supporting Evidence

Figures 38 shows the circuit running with converter 2 connected, with the anti-parallel bridge connected, and the transformer secondary connected to the SCR gates for the second converter in figure 39.

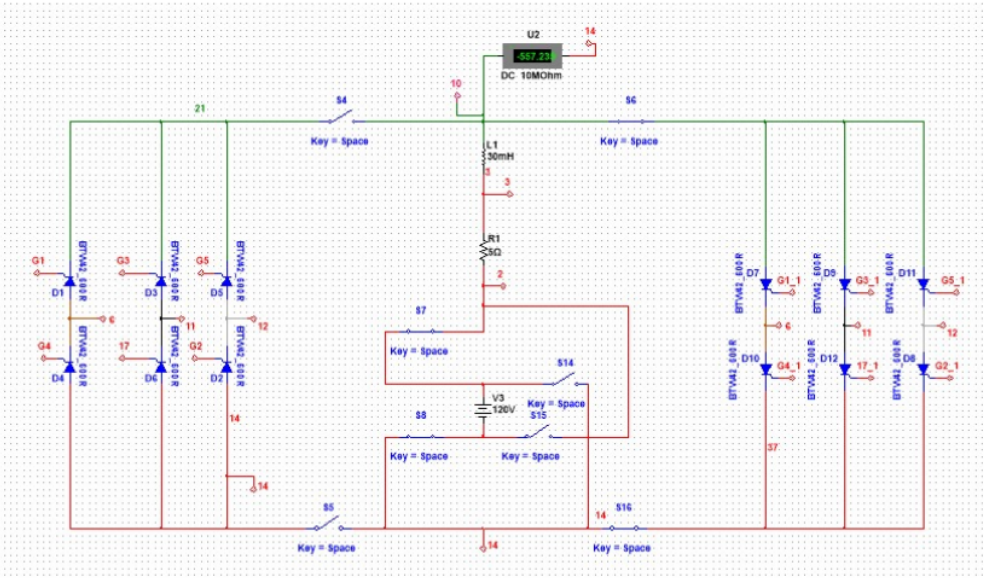


Figure 38 – Converter 2 Connected

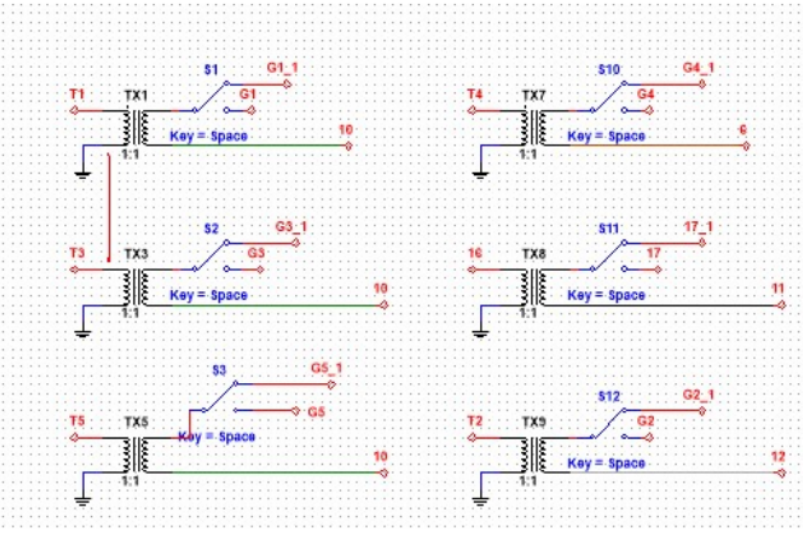
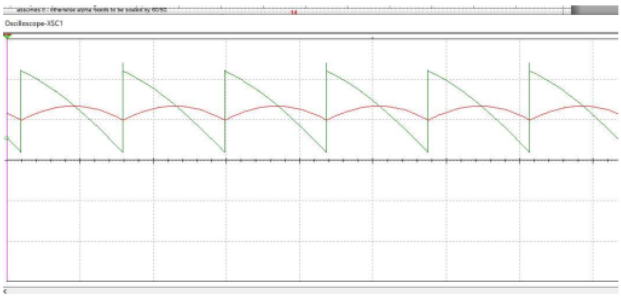


Figure 39 – Gate Triggers for Converter 2

Good cct design for dual converter adaption that includes the isolating transformers

Quadrant 1 Test for Dual Converter

Figure 40 shows the Multisim result for quadrant 1 operation. Both armature voltage and current are positive, the converter is in bridge 1 and the firing angle is below 90°. The motor is forward motoring.

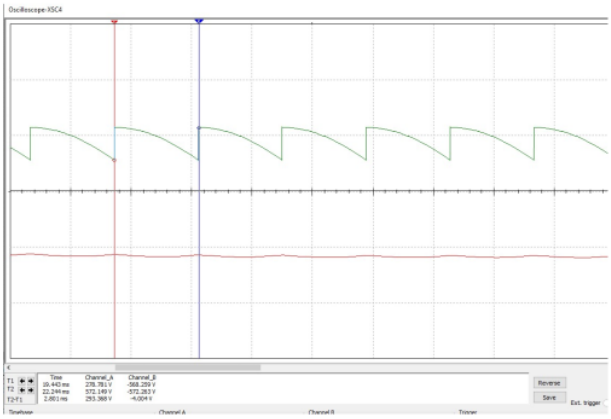


Good explanation and test

Figure 40 – Quadrant 1 Multisim Graph

Quadrant 2 Test for Dual Converter

Figure 41 shows the Multisim result for quadrant 2 operation. Both armature voltage and current are positive, the converter is in bridge 2 and the firing angle is above 90°. The motor is forward braking.



Good explanation and test result

Figure 41 – Quadrant 2 Multisim Graph

Quadrant 3 Test for Dual Converter

Figure 42 shows the Multisim result for quadrant 3 operation. Both armature voltage and current are positive, the converter is in bridge 2 and the firing angle is below 90°. The motor is reverse motoring.

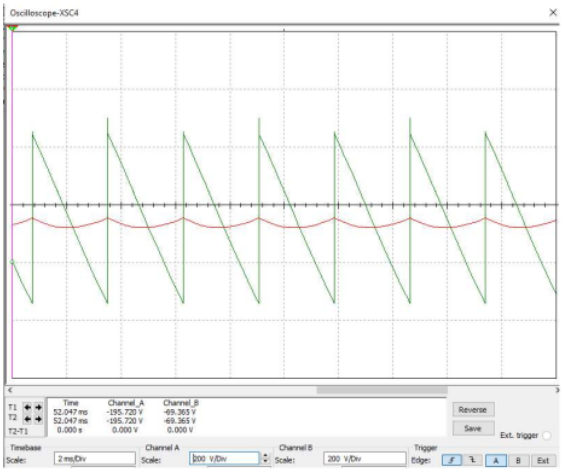


Figure 42 – Quadrant 3 Multisim Result

Good explanation and test result

Quadrant 4 Test for Dual Converter

Figure 43 shows the Multisim result for quadrant 4 operation. Both armature voltage and current are positive, the converter is in bridge 1 and the firing angle is above 90°. The motor is reverse braking.

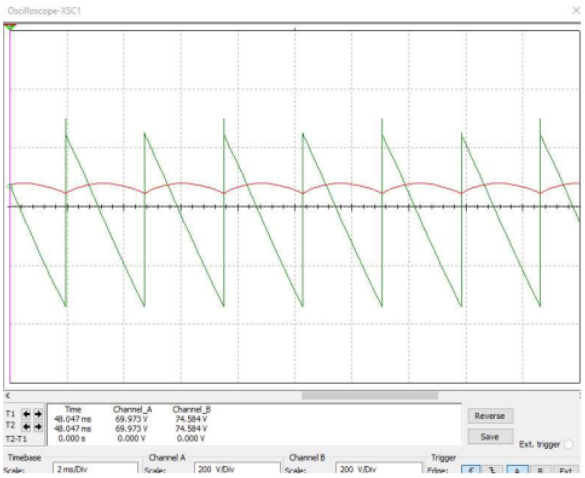


Figure 43 – Quadrant 4 Multisim Result

Good explanation and test result

Sim test for all 4 quadrants are explained with good results.Very good level of detail included.

8.3. Appendix for Section 5

8.3.1. Practical Task Supporting Evidence

Figure 44 shows the control cabinet for the AC-DC drive system. The control and protective circuitry can be seen, along with the two drives, PLC and HMI.

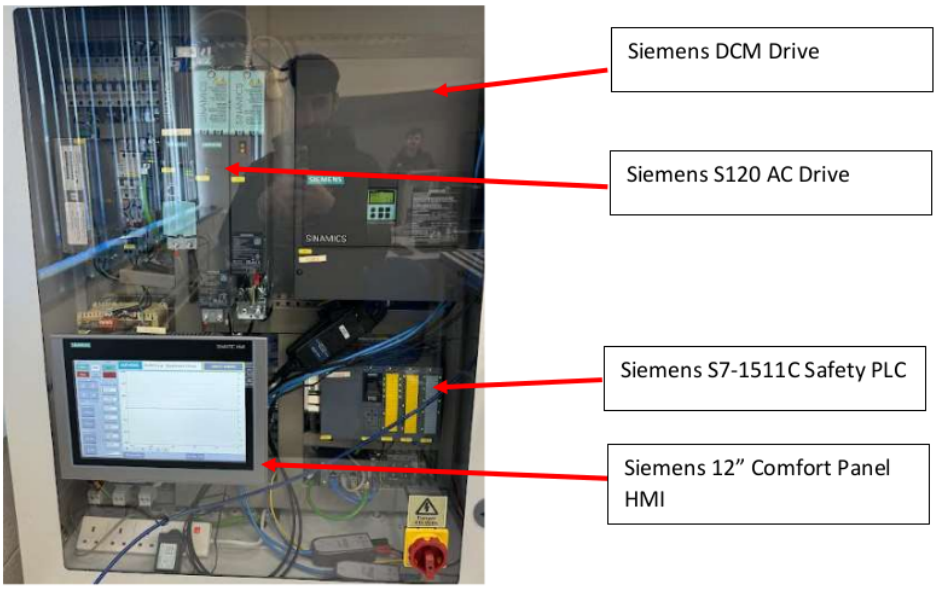


Figure 44 – Control Cabinet with Drives, PLC & HMI

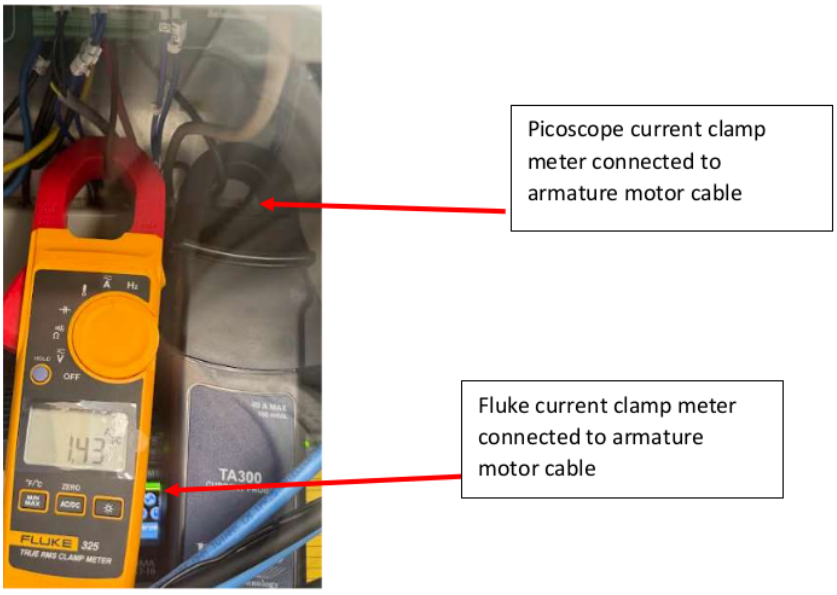


Figure 45 – Fluke & Picoscope Clamp Meters

8.3.2. Practical 4-Quadrant Operation Supporting Evidence

Quadrant 1 Results

Quadrant 1 results can be seen in figures 46-48, displaying the HMI, Picoscope and Fluke clamp meter results.

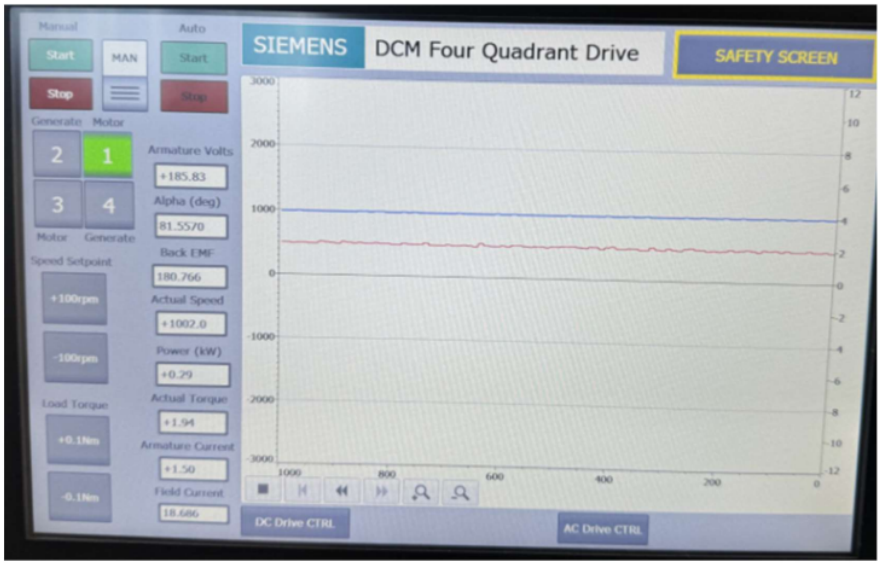
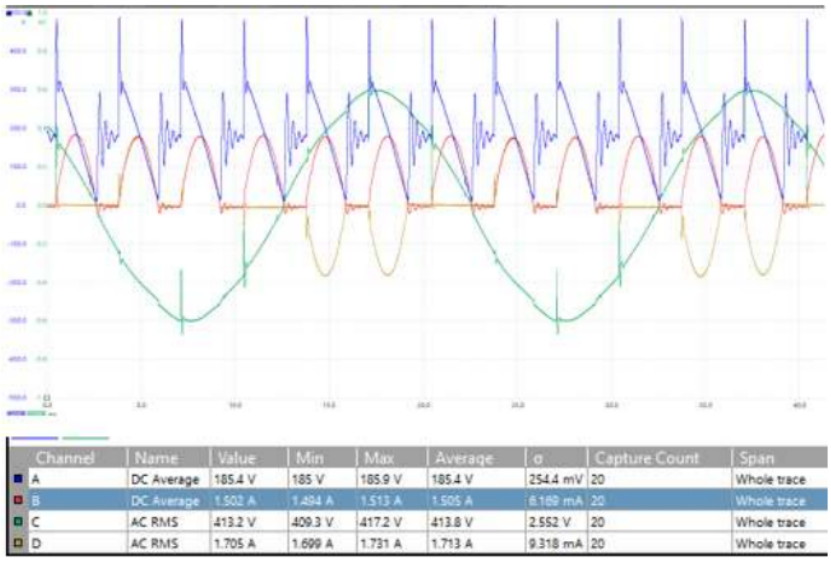


Figure 46 – Quadrant 1 HMI Result



Channel	Name	Value	Min	Max	Average	σ	Capture Count	Span
A	DC Average	185.4 V	185 V	185.9 V	185.4 V	254.4 mV	20	Whole trace
B	DC Average	1.502 A	1.494 A	1.513 A	1.505 A	6.189 mA	20	Whole trace
C	AC RMS	413.2 V	409.3 V	417.2 V	413.8 V	2.552 V	20	Whole trace
D	AC RMS	1.705 A	1.699 A	1.731 A	1.713 A	9.318 mA	20	Whole trace

Figure 47 – Quadrant 1 Picoscope Result

Good test result



Good test result

Figure 48 – Quadrant 1 Fluke Result

Quadrant 2 Results

Quadrant 2 results can be seen in figures 49-51, displaying the HMI, Picoscope and Fluke clamp meter results.

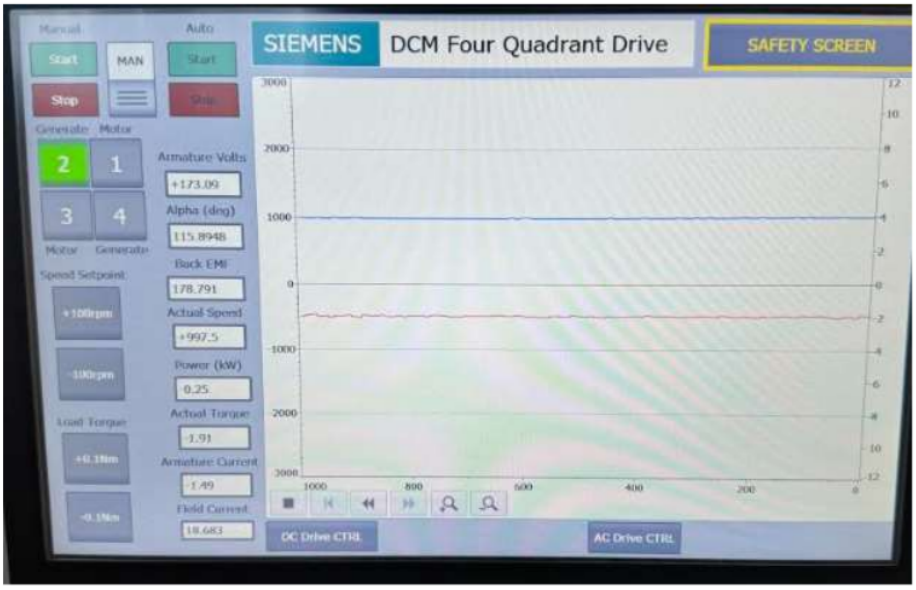
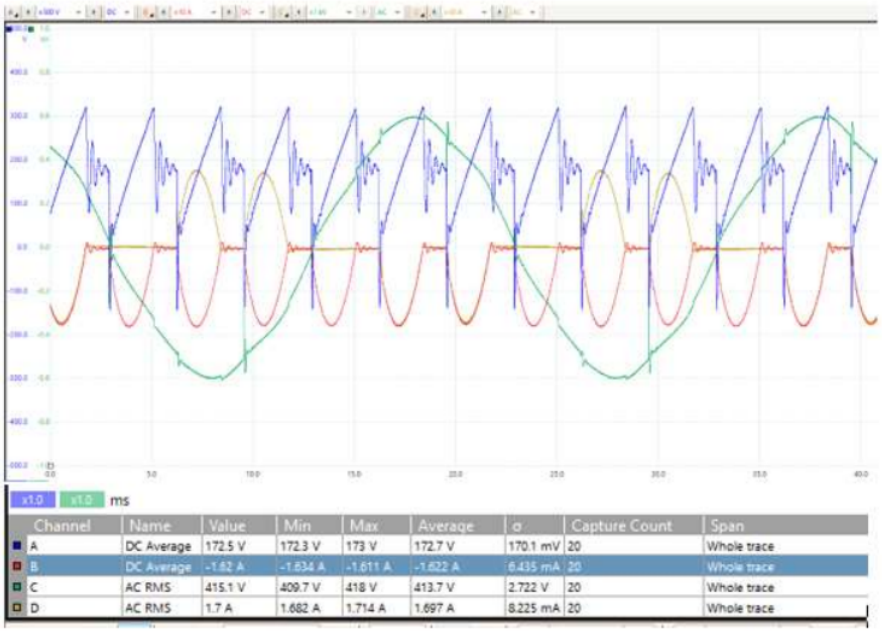


Figure 49 – Quadrant 2 HMI Result



Good test result

Figure 50 – Quadrant 2 Picoscope Result



Good test result

Figure 51 – Quadrant 2 Fluke Result

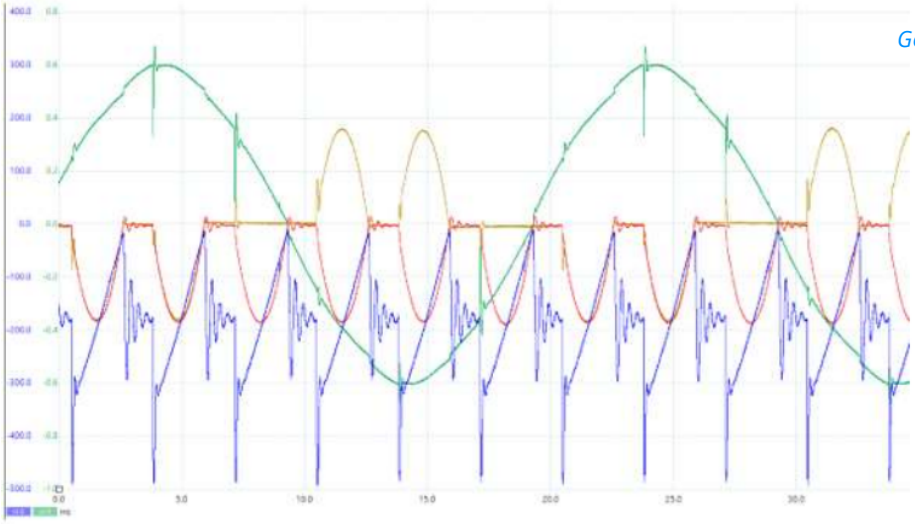
Quadrant 3 Results

Quadrant 3 results can be seen in figures 52-54, displaying the HMI, Picoscope and Fluke clamp meter results.



Figure 52 – Quadrant 3 HMI Result

Good test result



Channel	Name	Value	Min	Max	Average	σ	Capture Count
A	DC Average	-185.7 V	-186.3 V	-185.5 V	-185.8 V	213.5 mV	20
B	DC Average	-1.618 A	-1.634 A	-1.614 A	-1.622 A	5.421 mA	20
C	AC RMS	418 V	410.5 V	418.4 V	415 V	3.243 V	20
D	AC RMS	1.712 A	1.697 A	1.721 A	1.709 A	7.38 mA	20

Figure 53 – Quadrant 3 Picoscope Result



Good test result

Figure 54 – Quadrant 3 Fluke Result

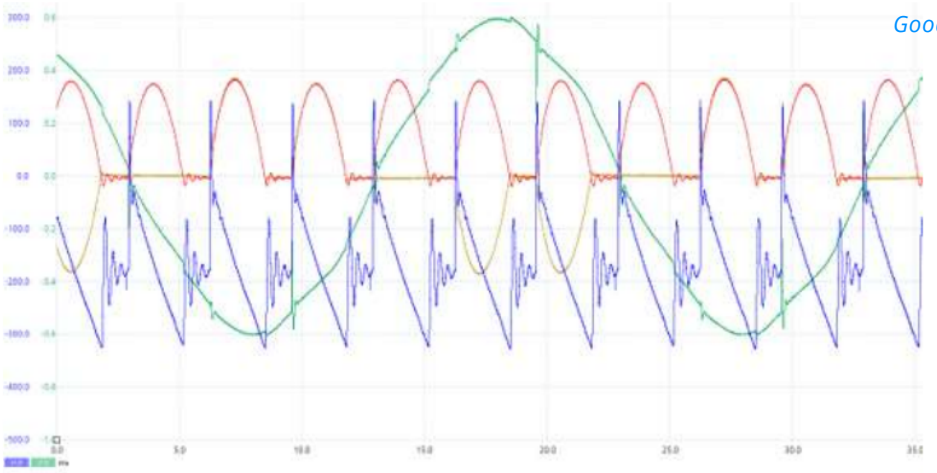
Quadrant 4 Results

Quadrant 4 results can be seen in figures 55-57, displaying the HMI, Picoscope and Fluke clamp meter results.



Figure 55 – Quadrant 4 HMI Result

Good test result



Channel	Name	Value	Min	Max	Average	σ	Capture Count
A	DC Average	-173.2 V	-173.7 V	-173 V	-173.4 V	172 mV	20
B	DC Average	1.592 A	1.587 A	1.604 A	1.597 A	5.219 mA	20
C	AC RMS	416.3 V	410.3 V	417.8 V	413.8 V	2.68 V	20
D	AC RMS	1.771 A	1.766 A	1.793 A	1.779 A	8.37 mA	20

Figure 56 – Quadrant 4 Picoscope Result

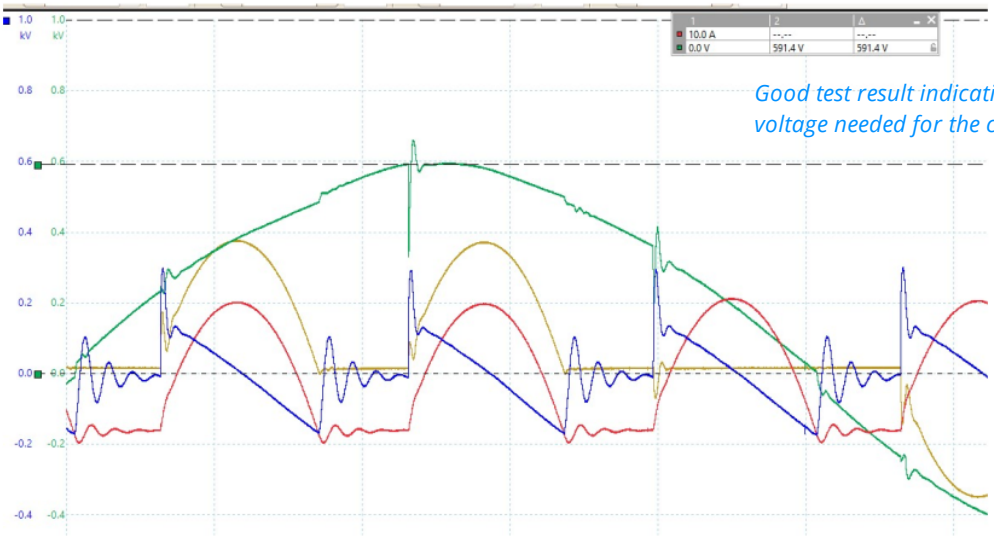


Figure 57 – Quadrant 4 Fluke Result

Good test result

8.3.3. Discontinuous Current Speed Setpoint Test Supporting Evidence

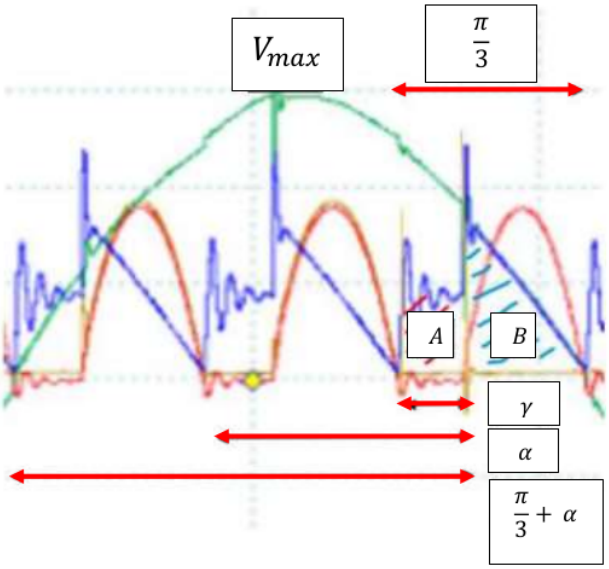
Figure 58 shows the Vmax value of 591.4V. The green cursor has been placed on the green waveform to find the voltage to be used in the armature voltage calculations.



Good test result indicating the max voltage needed for the calculation

Figure 58 – Vmax at 591V from Picoscope

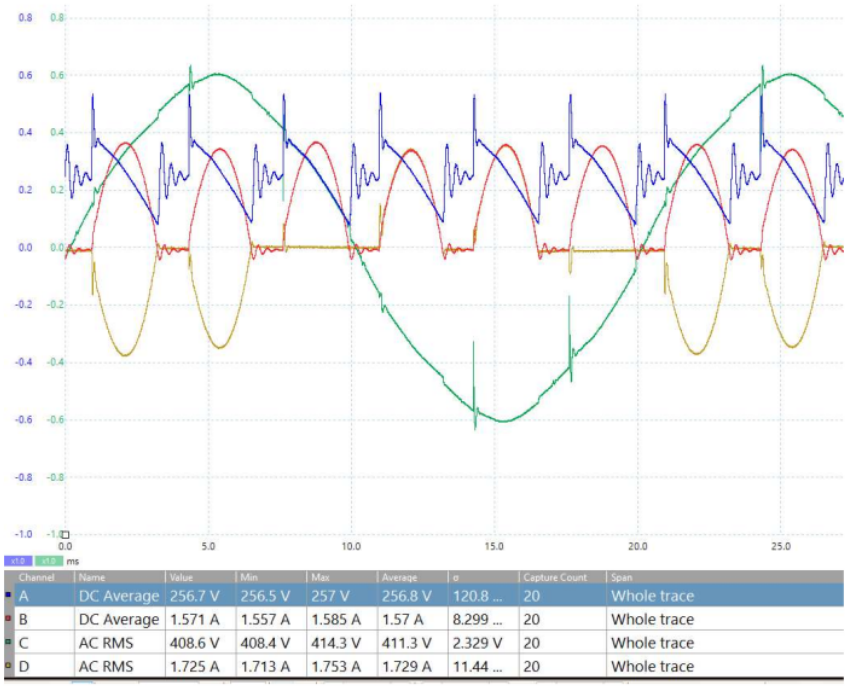
Figure 59 shows an annotated Picoscope graph, with the relevant mathematical terms labelled, with areas A and B shaded in.



This is excellent here

Figure 59 – Picoscope Graph Annotated for Mathematical Terms

1400RPM Results



Channel	Name	Value	Min	Max	Average	σ	Capture Count	Span
A	DC Average	256.7 V	256.5 V	257 V	256.8 V	120.8 ...	20	Whole trace
B	DC Average	1.571 A	1.557 A	1.585 A	1.57 A	8.299 ...	20	Whole trace
C	AC RMS	408.6 V	408.4 V	414.3 V	411.3 V	2.329 V	20	Whole trace
D	AC RMS	1.725 A	1.713 A	1.753 A	1.729 A	11.44 ...	20	Whole trace

Figure 60 – 1400RPM Picoscope Results

Good test result

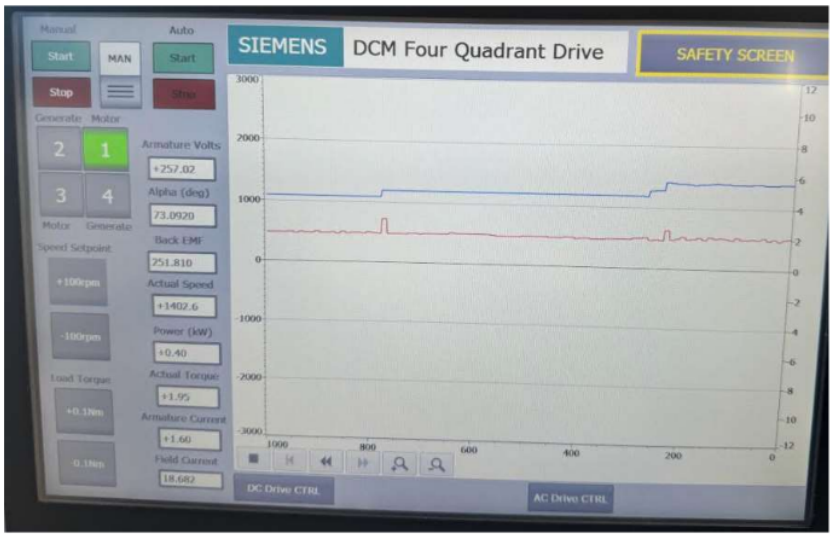


Figure 61 – 1400RPM HMI Result

Table 16 shows the values to be used in the 1400RPM calculations.

Parameters	Value
E (Back EMF)	251.81V
α (Firing Angle)	73.09°
Vmax	591V

Table 16 – Values for 1400RPM Calculations

Good use of table of results

The α must be converted into radians:

$$\alpha = 73.09 \times \frac{\pi}{180} = 1.27$$

Equation 21 – 1400RPM α Calculation

Area A:

$$Area\ A = E\left(\alpha - \frac{\pi}{3}\right) = 251.81(1.27 - 1.047) = 56.15V$$

Equation 22 – 1400RPM Area A Calculation Result

Area B:

$$Area\ B = 591(1 + \frac{1}{2}\cos(1.27) - \frac{\sqrt{3}}{2}\sin(1.27)) = 189.71V$$

Equation 23 – 1400RPM Area B Calculation Resul

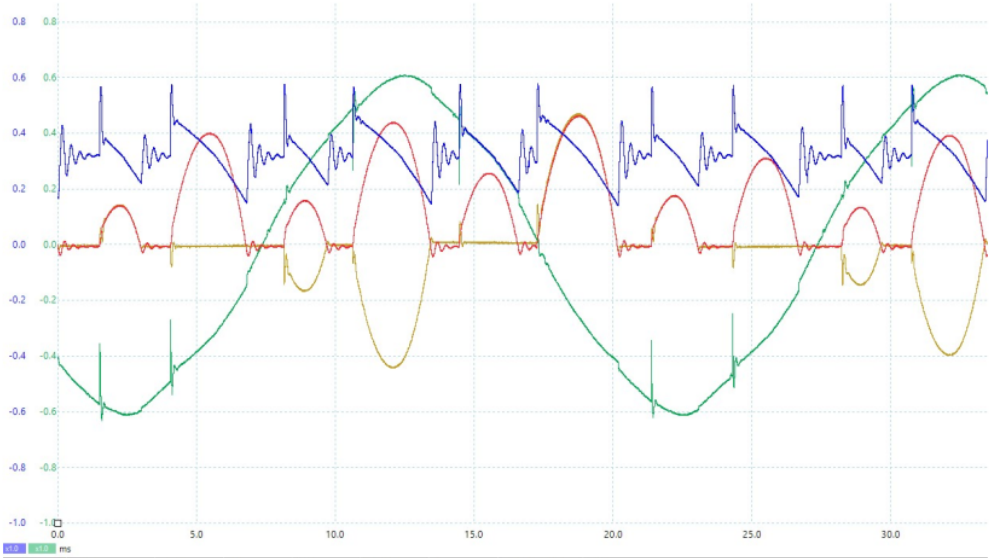
V_{mean}:

$$V_{mean} = \frac{56.15 + 189.71}{\pi/3} = 234.78V$$

Good work

Equation 24 – 1400RPM Vmean Calculation Result

1800RPM Results



Channel	Name	Value	Min	Max	Average	σ	Capture Count	Span
A	DC Average	328 V	326.6 V	328.6 V	327.8 V	730.3 ...	6	Whole trace
B	DC Average	1.536 A	1.445 A	1.623 A	1.523 A	66.1 mA	6	Whole trace
C	AC RMS	412.2 V	408.8 V	415.5 V	411.7 V	3.048 V	6	Whole trace
D	AC RMS	1.856 A	1.722 A	1.916 A	1.817 A	81.34 ...	6	Whole trace

Figure 62 – 1800RPM Picoscope Result

Good test result



Figure 63 – 1800RPM HMI Result

Table 17 shows the values to be used in the 1800RPM calculations.

Parameters	Value
E (Back EMF)	324.35V
α (Firing Angle)	60.74°
Vmax	591V

Table 17 – 1800RPM Calculation Values

Good use of table of results

The α must be converted into radians:

$$\alpha = 60.74 \times \frac{\pi}{180} = 1.06$$

Equation 25 – 1800RPM α Calculation Result

Area A:

$$Area\ A = E\left(\alpha - \frac{\pi}{3}\right) = 324.35(1.06 - 1.047) = 4.22V$$

Equation 26 – 1800RPM Area A Calculation Result

Area B:

$$Area\ B = 591(1 + \frac{1}{2}\cos(1.06) - \frac{\sqrt{3}}{2}\sin(1.06)) = 288.97V$$

Equation 27 – 1800RPM Area B Calculation Result

V_{mean}:

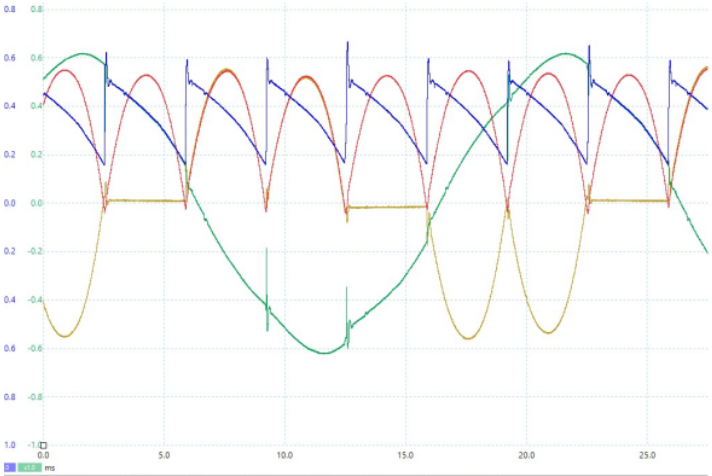
$$V_{mean} = \frac{4.22 + 288.97}{\pi/3} = 279.98V$$

Good work

Equation 28 – 1800RPM Vmean Calculation Result

8.3.4. Torque Setpoint Test at Constant Speed Supporting Evidence

4.5Nm Results



Channel	Name	Value	Min	Max	Average	σ	Capture Count	Span
A	DC Average	370.3 V	368.5 V	370.6 V	369.6 V	722 mV	20	Whole trace
B	DC Average	3.581 A	3.398 A	3.618 A	3.498 A	68.5 mA	20	Whole trace
C	AC RMS	416.7 V	411.3 V	416.7 V	414 V	2.236 V	20	Whole trace
D	AC RMS	3.27 A	3.07 A	3.27 A	3.165 A	64.8 mA	20	Whole trace

Good test result

Figure 64 – 4.5Nm Picoscope Result

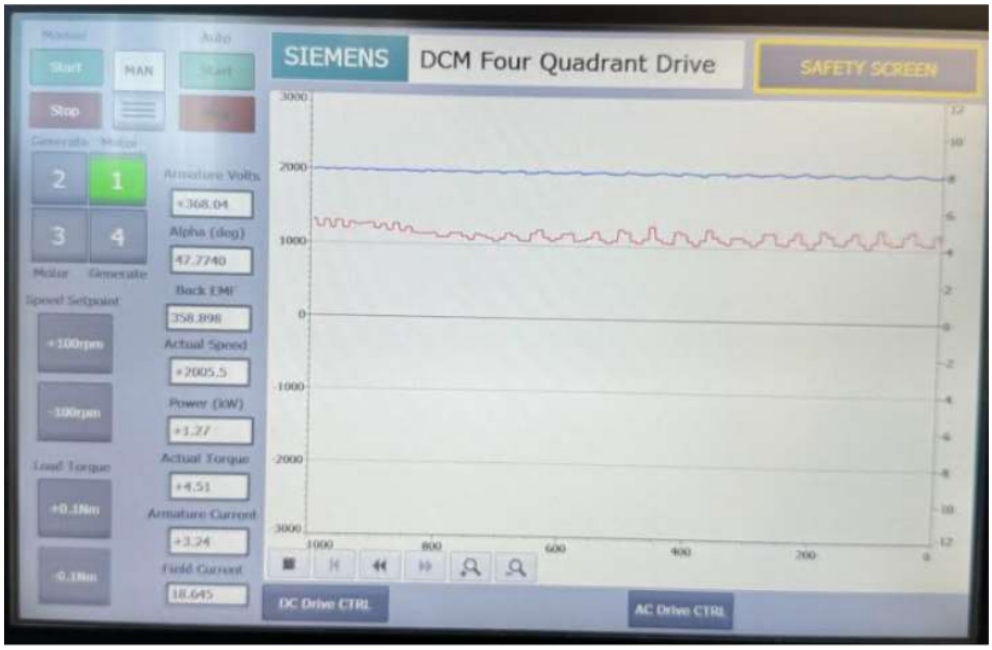
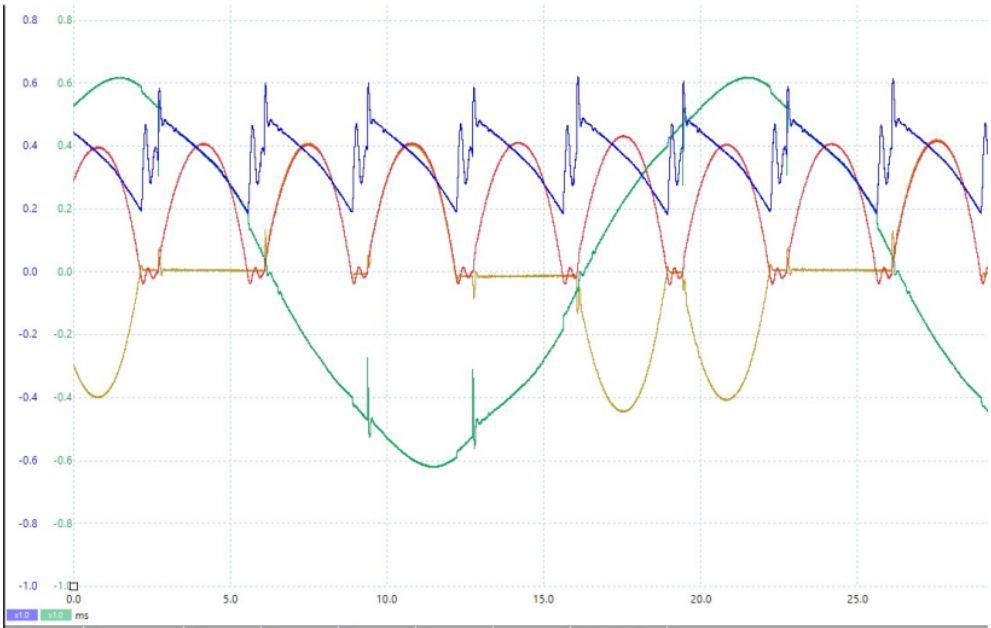


Figure 65 – 4.5Nm HMI Result

3Nm Results



Channel	Name	Value	Min	Max	Average	σ	Capture Count	Span
A	DC Average	366.1 V	366.1 V	367.2 V	366.8 V	289.6 ...	20	Whole trace
B	DC Average	2.36 A	2.335 A	2.395 A	2.366 A	14 mA	20	Whole trace
C	AC RMS	416.5 V	411.7 V	417.4 V	414.3 V	2.014 V	20	Whole trace
D	AC RMS	2.314 A	2.29 A	2.321 A	2.308 A	8.812 ...	20	Whole trace

Figure 66 – 3Nm Picoscope Result

Good test result



Figure 67 – 3Nm HMI Result

2017197

GRADEMARK REPORT

FINAL GRADE

GENERAL COMMENTS

89 /100

PAGE 1

PAGE 2

PAGE 3

Text Comment. A very detailed and professional table of contents

PAGE 4

PAGE 5

Text Comment. An extensive and detailed table of figures

PAGE 6

Text Comment. Good extensive use of tables to order and evaluate results

PAGE 7

Text Comment. Good use of tables to logically order results

PAGE 8

Text Comment. Good points made here

Text Comment. Good observation

Text Comment. Good points made

Text Comment. A very well written summary

PAGE 9

Text Comment. Good plan with significant details

PAGE 10

Text Comment. Internal control loops are identified here and with a good supporting diagram

Text Comment. Good significant point

Text Comment. Very good work with good ref source

PAGE 11

Text Comment. This is very good work with PID control and purpose of error explained

Text Comment. Good points

Text Comment. Good work with purpose of firing angles explained

Text Comment. Good point

Text Comment. A very significant point

Text Comment. Good explanation

PAGE 12

Text Comment. Good relevant diagram

PAGE 13

Text Comment. Good explanation with very good relevant diagram and ref source

Text Comment. Good use of table to identify speed and torque in 4 quadrant drive scenario

PAGE 14

Text Comment. Significant events for speed and armature current identified

Text Comment. A very good detailed diagram with good annotations.

PAGE 15

Text Comment. Good significant point

Text Comment. A good level of detail included in the spec here and good use of table

PAGE 16

Text Comment. Good work

PAGE 17

Text Comment. Excellent work here

PAGE 18

Text Comment. Very good comparison table that highlights significant advatages for DC motors

Text Comment. Chopper fed drives should be included in the comparison

PAGE 19

Text Comment. Excellent annotated sim diagram that identifies key features

PAGE 20

Text Comment. Good significant point

Text Comment. Good work

Text Comment. Correct equation is identfied

Text Comment. Good explanation

PAGE 21

Text Comment. Good test result

Text Comment. Good result

PAGE 22

Text Comment. Good table of results with error identified

Text Comment. Good argument for error correlation

Text Comment. Good explanation of results

PAGE 23

Text Comment. Good point

Text Comment. Good detailed explanation

Text Comment. A very good annotated sim cct diagram

PAGE 24

Text Comment. Excellent work

PAGE 25

Text Comment. Good annotated sim results

Text Comment. Excellent work here

PAGE 26

Text Comment. Good explanation and supporting diagram

PAGE 27

Text Comment. Good detailed explanation and annotated diagram

PAGE 28

Text Comment. Excellent annotated results screenshot that identifies the 4 quadrant components orientation. This result agrees with the literature

PAGE 29

Text Comment. Excellent set of results presented

Text Comment. Good use of table to identify key components on graphs

PAGE 30

Text Comment. Good table of comparison

Text Comment. Good set of results that follow the 4 quadrant operation procedure

PAGE 31

Text Comment. Good explanation

PAGE 32

Text Comment. Excellent work here

PAGE 33

Text Comment. Good explanation

Text Comment. Good test result

PAGE 34

Text Comment. Good table of results

PAGE 35

Text Comment. Good work

Text Comment. Very good explanation and use of tables for results

PAGE 36

Text Comment. Good ref to appendix

Text Comment. Good table of values for comparison

Text Comment. Good explanation

Text Comment. Very good argument that agrees with theory

PAGE 37

Text Comment. Good test results with values needed for calculations

Text Comment. Formula is identified

PAGE 38

Text Comment. Good work

Text Comment. Formula check proves result for Ra

PAGE 39

Text Comment. Good work

Text Comment. Good work

Text Comment. Good work here. Formula has been identified and used to find constants related to the motor.

PAGE 40

Text Comment. Good explanation of procedure and test result for continuous current

Text Comment. Good values obtained

PAGE 41

Text Comment. Excellent work

Text Comment. Acceptable errors

Text Comment. Very good explanation that includes significant points

PAGE 42

Text Comment. Good points included

Text Comment. Good significant points form research findings

Text Comment. This is a good valid point

Text Comment. Good valid points covered here

Text Comment. Good points included

PAGE 43

Text Comment. Purpose of adapted drive to accomodate 4 quadrant operation

Text Comment. Good valid points

Text Comment. Good points covered

Text Comment. Good recommendation

Text Comment. A very good recommendation

PAGE 44

PAGE 45

Text Comment. Good number of ref sources

PAGE 46

Text Comment. Good point

Text Comment. Good significant point here

Text Comment. Good point

Text Comment. Good explanation with relevant ref source

Text Comment. Good explanations with significant points made and good supporting diagrams

PAGE 47

Text Comment. Good explanation and supporting image

Text Comment. Good supporting image

PAGE 48

Text Comment. Good explanation and diagram

Text Comment. Significant points ar highlighted and explained

PAGE 49

PAGE 50

Text Comment. Key features of drive are identified

PAGE 51

Text Comment. Good supporting research with very good level of detail

PAGE 52

Text Comment. Good example that identifies the need for 4 quadrant operation

PAGE 53

Text Comment. Good test result

PAGE 54

Text Comment. Good test that identifies quadrant 4 opertion for ths single converter drive

PAGE 55

Text Comment. Good test result

PAGE 56

Text Comment. Good test result

PAGE 57

Text Comment. Good test result

PAGE 58

Text Comment. Good test result

PAGE 59

Text Comment. Good cct design for dual converter adaption that includes the isolating transformers

PAGE 60

Text Comment. Good explanation and test

Text Comment. Good explanation and test result

PAGE 61

Text Comment. Good explanation and test result

Text Comment. Good explanation and test result

Text Comment. Sim test for all 4 quadrants are explained with good results.Very good level of detail included.

PAGE 62

PAGE 63

Text Comment. Good test result

PAGE 64

Text Comment. Good test result

PAGE 65

Text Comment. Good test result

PAGE 66

Text Comment. Good test result

PAGE 67

Text Comment. Good test result

PAGE 68

Text Comment. Good test result

PAGE 69

Text Comment. Good test result

PAGE 70

Text Comment. Good test result

PAGE 71

Text Comment. Good test result indicating the max voltage needed for the calculation

Text Comment. This is excellent here

PAGE 72

Text Comment. Good test result

PAGE 73

Text Comment. Good use of table of results

Text Comment. Good work

PAGE 74

Text Comment. Good test result

PAGE 75

Text Comment. Good use of table of results

Text Comment. Good work

PAGE 76

Text Comment. Good test result

PAGE 77

Text Comment. Good test result

GRADING FORM: NEW CSG-RUBRIC

AERON SMITHAM

0

1. ENGAGEMENT WITH LITERATURE

17/20

Research is extensive with good quality ref sources used. The level of detail is excellent and demonstrates an understanding of requirements. There are excellent key technical features included with relevant diagrams. An example application of the chopper drive option could have been included.
The research is excellent.

2. KNOWLEDGE AND UNDERSTANDING

18/20

Theory from research has been proven using test and analysis methods in the tasks.
Implementation is very organised and all stages are explained in detail. Good comparison methods using tables are used for evaluation purposes.
Simulated methods have been carried out successfully with very good technical explantions relating to theory.
Practical tasks have been carried out methodically and using tables of results for evaluation.
Thorough testing has been carried out with an abundance of well presented evidence that is clearly referenced in appendix.
An excellent level of understanding demonstrated.

3. COGNITIVE AND INTELLECTUAL

Simulation of full wave controlled rectfication has been achieved and tests have been carried out.
Tables of results have been presented in good order and results have been evaluated.
Adapted sim cct test for 4 quadrant operation has been carried out and results evlauated against research findings.
All practical test requirements have been carried out, constant speed with discontinuous current and constant torque with continuous current.
Results are presnted using tables and explained in detail.
A very good conclusion that points out key features of the tasks carried out and the results.
Good recommendaions are included, one of which is very relevant and a good point for future reference.
Results for sim and prac were compared to calculated values and tables used to present findings.

18/20

4. PRACTICAL APPLICATION

Practical application of simulated ccts has been carried out using very good methods and real problems have been resolved.
The designs indicate a progression from the full wave controlled to the adapted dual converter for 4 quadrant operation. This is explained in very good detail and emphasises the high level of understanding of the procedures.

18/20

Practical application showed initiative and evidence inculded demonstrates the initiatives with the tasks.
Results were taken from a wide range of tests carried out for speed and torque.

5. TRANSFERABLE SKILLS



An excellent report with real quality content. References to appendix is excellent and very detailed.

18/20